Mon. Not. R. Astron. Soc. **000**, 1–14 (1997) Printed 4 September 1998 (MN LaTeX style file v1.4)

CCD photometry of variable stars in the Magellanic Clouds – V. The eclipsing binaries HV 1620 and HV 2241

J.D. Pritchard,[1] W. Tobin,[1] M. Clark[1] and E.F. Guinan[2]
[1] *Mount John University Observatory and Department of Physics & Astronomy, University of Canterbury, Private Bag 4800, Christchurch, New Zealand*
[2] *Department of Astronomy & Astrophysics, Villanova University, Villanova, PA 19085, U.S.A.*

Accepted 1998 January ??. Received 1997 November 7

ABSTRACT
Using improved techniques, high-quality CCD $uvbyVI_C$ photometry has been obtained for the 14-th magnitude eclipsing binaries HV 1620 in the Small Magellanic Cloud (SMC) and HV 2241 in the Large Magellanic Cloud (LMC). *IUE* ultraviolet spectrophotometry was also obtained. These data have been analyzed using the Wilson & Devinney synthetic light-curve code and Kurucz model atmospheres. Both systems are semi-detached and appear to have undergone mass exchange. In HV 1620 the mass ratio and the effective temperatures of the primary and secondary are $q = M_2/M_1 = 0.68 \pm 0.03$, $T_{\rm eff,1} = 33\,000{\pm}4\,500$ K and $T_{\rm eff,2} = 24\,400{\pm}3\,500$ K. The corresponding values for HV 2241 are 0.53 ± 0.01, $27\,000{\pm}3\,000$ K and $20\,200{\pm}1\,500$ K. Using the radial-velocity curves obtained by Niemela & Bassino (1994) with a 1-m telescope, we find that both systems are massive, as expected. Reddening considerations suggest both systems may lie towards the rear of their respective Clouds.

Key words: binaries: eclipsing – stars: early-type – stars: fundamental parameters – stars: individual: HV 982, HV 1620, HV 2241 – Magellanic Clouds

1 INTRODUCTION

The observational study of double-lined eclipsing binaries provides the primary source of accurate fundamental stellar data—in particular, the individual masses and radii of both component stars of the system. For extragalactic eclipsing binaries, the distance moduli are also of extreme interest (e.g. Guinan, Bradstreet & DeWarf 1996, Hilditch 1996, Paczyński 1997). A programme of CCD photometry of eclipsing binaries in the Magellanic Clouds is underway at the Mount John University Observatory, Lake Tekapo, New Zealand (MJUO) and results from the first observational campaign in 1990 have been published (West, Tobin & Gilmore 1992, Watson et al. 1992, Tobin et al. 1993a, Duncan et al. 1993).

In the 1990 campaign, unguided BVI images were obtained with a 0.6-m Boller & Chivens Cassegrain telescope using broad-band filters which were changed manually. Instrumental magnitudes were extracted using ROMAFOT (Buonanno & Iannicola 1989, and references therein). ROMAFOT has the advantage of allowing each step in the reduction process to be monitored, but has the disadvantage of employing a circularly-symmetric Point Spread Function (PSF). The observed PSFs were not circularly-symmetric and this undoubtedly increased the photometric uncertainty. Further, the adopted correction for response non-uniformities across the field of the CCD ('flat fielding') was recognised as problematic at the several-percent level (e.g. Tobin 1993). Thus differential photometry obtained with the (German-mounted) telescope tube positioned above the polar axis required a systematic offset to be brought into agreement with that obtained with the telescope tube beneath the polar axis. The precision obtained for the differential photometry was ∼1-3 per cent, while absolute values of the targets' magnitudes were uncertain at the 0.1-mag level.

Andersen (1991) has emphasized that the highest quality data are essential for meaningful discrimination between stellar structure models that differ in respect to items of current debate, such as helium abundance, opacity, mixing length and the overshooting parameter. Uncertainties in radius and mass must be no larger than ∼1 and ∼2 percent respectively.

We have therefore endeavoured to improve our observation and reduction techniques and procedures with the aim of achieving photometry of the quality required by the above demands. We have moved to a larger telescope and a computer-controlled photometer head that permits guided observations and automatic filter selection. Flat-fielding arrangements have been improved. At shorter wavelengths intermediate-band filters from the better-calibrated Strömgren system have been adopted; this also reduces the

© 1997 RAS

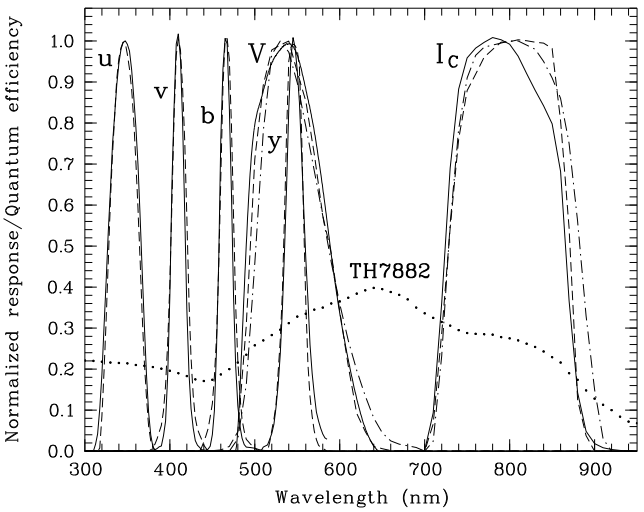

Figure 1. Achieved normalized response functions (full lines) compared to the *uvby* and VI_C system responses (dashed lines) given by Olson (1974) and Lamla (1982) or inferred from Matsushima (1969) and Bessell (1979, for a photocathode at $-10°$C). These V and I_C responses differ only slightly from the improved ones tabulated by Bessell (1990, dot-dashed lines). Also shown is the CCD quantum efficiency claimed by Photometrics (dots). The achieved responses, $S(\lambda)$, are the product of the measured filter transmissions and the quantum efficiency of the detector. The corresponding mean wavelengths $\overline{\lambda} = \int \lambda S(\lambda)\mathrm{d}\lambda / \int S(\lambda)\mathrm{d}\lambda$ of the filters are: 346.6, 410.0, 465.9, 548.2, 544.2 and 794.6 nm. The u and V filters are glass alone; interference cavities are present in the others.

effects of colour mismatch between programme stars and flat-field lamps.

Finally, for extraction of instrumental magnitudes, we have employed DAOPHOT II (Stetson 1987) which allows for non circularly-symmetric PSFs. We have tested our new procedures with observations of the eclipsing binaries HV 1620 and HV 2241. These stars were selected as test objects because they are relatively bright ($V \simeq 14.5$ and 13.5, respectively) and have some published photoelectric photometry (Herczeg 1982, Davidge 1987, 1988) and spectroscopy (Niemela & Bassino 1994, and references therein). Some estimate of the effect of crowding on our photometry is possible because HV 2241 is in a relatively empty field whereas HV 1620 is in a more crowded one. Finally HV 1620 is in the Small Magellanic Cloud (SMC) whereas HV 2241 is in the Large Magellanic Cloud (LMC). This is observationally convenient in that when one star is near lower culmination, the other is not. In addition, stars in the two Clouds have significantly different metallicities both with respect to the Milky Way and with respect to each other. HV 1620 and HV 2241, however, are not well-detached systems which can be analyzed with a simple synthetic light-curve code such as EBOP (Etzel 1981, 1993), nor can they furnish the best comparisons with models of single-star evolution. For analysis we have adopted the Wilson & Devinney synthetic light curve code (Wilson 1979, hereafter 'WD'), which is based on Roche equipotentials, modifying it to incorporate fluxes from Kurucz model atmospheres of metallicity appropriate to the Clouds (Kurucz 1993).

Analyses of earlier data have been carried out for HV 1620 by Davidge (1988), for HV 2241 by Russell (1956) and Davidge (1987), and for both stars by Niemela & Bassino (1994).

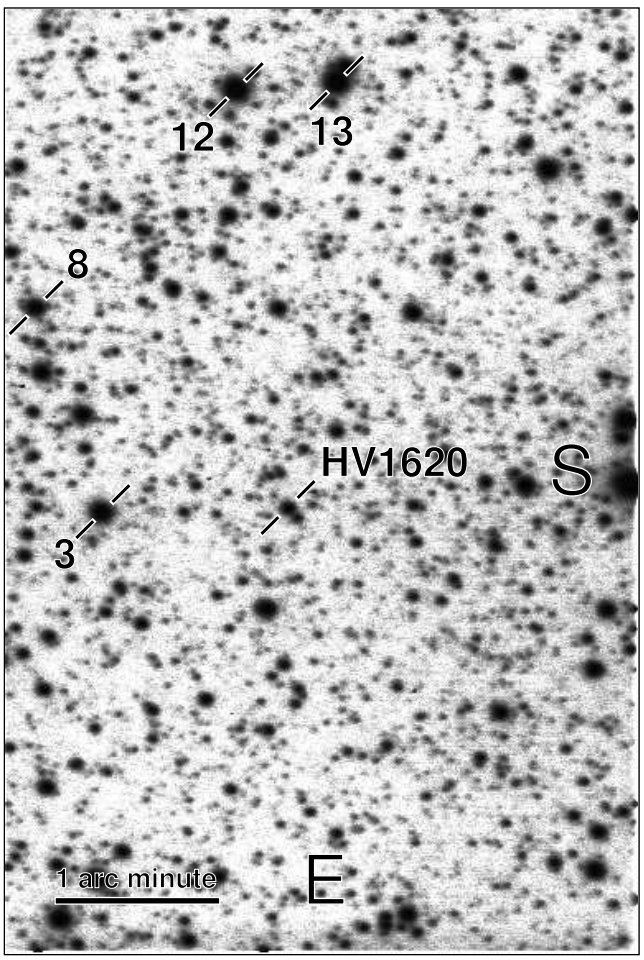

Figure 2. An I_C-band image showing the adopted field positioning for HV 1620 in the SMC. The comparison signal for differential photometry was obtained by adding fluxes from stars 8 and 12; a check signal came from adding stars 3 and 13, except for V where stars 8 and 3 were used as comparison and check respectively since stars 12 and 13 were usually saturated in typical V exposures. An accurate position for HV 1620 was obtained by differential measurement with respect to adjacent stars in the Cape Photographic Catalogue 1950.0 (Stoy 1966), in the way described in Paper III (Tobin et al. 1993a). The 2000.0 coordinates are RA $0^{\mathrm{h}}54^{\mathrm{m}}36^{\mathrm{s}}.64 \pm 0^{\mathrm{s}}.2$, Dec. $-72°32'04''.8 \pm 0''.1$.

2 INSTRUMENTATION, OBSERVATIONS AND REDUCTIONS

Full details of the procedures summarized in this section can be found in Pritchard (1997).

2.1 Optical photometry

Photometric observations of HV 1620 and HV 2241 were made between 1992 November and 1995 October using the McLellan Cassegrain 1-m telescope at MJUO in its f/7.7 configuration in conjunction with the new CCD photometer

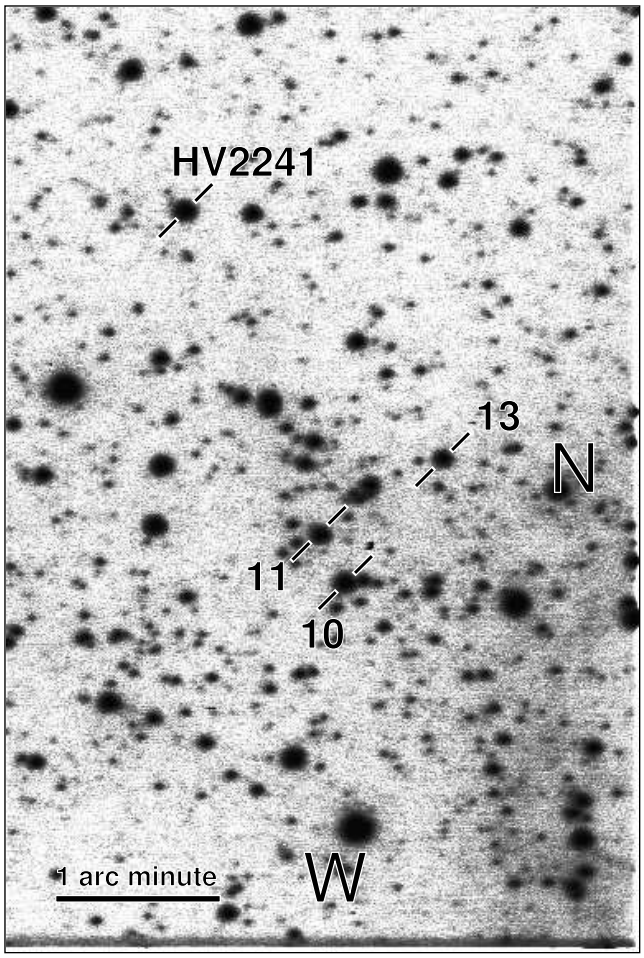

Figure 3. An I_C-band image showing the adopted field positioning for HV 2241 in the LMC. Star 10 provided the comparison for differential magnitudes; addition of the fluxes from stars 11 and 13 gave a check signal. The 2000.0 coordinates of HV 2241 were measured to be RA $4^h57^m15\overset{s}{.}84\pm0\overset{s}{.}24$, Dec. $-66°33'56\overset{''}{.}0\pm0\overset{''}{.}6$.

head (Tobin et al. 1993b). The detector was the Photometrics PM3000 cryogenic CCD system which incorporates a Thomson TH7882 CDA chip with an array of 576 × 384 square pixels. The chip is overcoated with Metachrome II for blue and ultraviolet sensitivity. The pixels' 23 μm size projects to $0\overset{''}{.}62$ on the sky. The system inverse gain and base-level noise were 4.31±0.06 e^-/ADU and 7.1±0.1 e^- respectively (Tobin 1992).

Prior to 1993 March, observations were made only in V, using a filter composed of 2 mm of Schott GG495 filter glass oiled to 3 mm of BG39. Thereafter observations were also made in Strömgren *uvby* and Cousins I_C using imaging-quality glass or interference filters manufactured by Omega Optical Inc. of Brattleboro, Vermont. These filters were specified such that the product of their transmission and the detector quantum efficiency would yield the responses for the Strömgren or Cousins VI_C systems, as explained in the caption to Figure 1. The I_C filter, in particular, included an interference element to provide the required steep transmission cut-off at ∼870 nm. In addition, these filters (and the V filter) were packed to similar thicknesses so that telescope refocussing was not necessary between filters. Figure 1 compares the required responses to those achieved.

Flat-field images were obtained by pointing the McLellan telescope at an illuminated, plasticized screen attached to the inside of the dome. Scattered light, which it is believed contributed to the low-frequency flat-fielding difficulties experienced in the 1990 campaign, was markedly reduced by black painting the dome screen down to the size of the telescope beam and more especially by adding sharpened annuli inside the skirt and chimney baffles of the telescope. However we have not as yet succeeded in testing the flatness of corrected images through the polynomial fitting procedure suggested by Djorgovski (1984) and recently demonstrated by Manfroid (1995). We therefore always attempted to position each programme or standard star at the same location on the CCD chip to within ±3 pixels. In this way, the effect of any flat-field warp was removed from absolute photometry and was converted into a systematic effect for differential photometry, affecting differential magnitudes by a constant (though unknown) offset. Figures 2 and 3 show the adopted field positions for the programme stars. Integration times for the programme-star exposures were mostly 1200 s for u, v and b, 700 s for y, 400 s for V and 200 s for I_C.

2.1.1 Differential photometry

Differential photometry was obtained during 38 and 14 nights for HV 1620 and HV 2241 respectively. Observing conditions varied widely with FWHM seeing ranging from 2 to 8 arcsec. Instrumental magnitudes were extracted using DAOPHOT II (Stetson 1987) within the integrated environment for reduction and analysis provided by the Munich Image Data Analysis System, MIDAS (e.g. Banse et al. 1987, Grosbøl 1989). MIDAS was run in Christchurch on the University of Canterbury's VAX cluster under VAX/VMS (versions 91MAY and 92NOV), and on the UNIX cluster under SunOS 5.4 (94NOV).

For each CCD image, DAOPHOT constructs a hybrid analytical/empirical PSF to selected stars. Instrumental magnitudes are determined from integration of this PSF. Since DAOPHOT can take account of the arbitrary, asymmetric nature of real PSFs, its instrumental magnitudes should be superior to those from ROMAFOT. For HV 1620 in I_C, iterative use of DAOPHOT was necessary to remove the signal from the fainter star ∼6 arcsec to the south east before final PSF fitting.

Despite the fact that the adopted CCD fields of view for both HV 1620 and HV 2241 contain several hundred stars, perhaps the most difficult aspect of obtaining high-precision CCD differential photometry was finding appropriate comparison and check stars of sufficient photometric stability within the field of view. Preliminary field surveys for both stars were made in filters approximating U and I_C. The field positions (Figures 2 and 3) attempt to include as many stars as possible with ultraviolet brightnesses comparable to the target. The stability of 12 stars was examined for HV 1620, while 17 were investigated for HV 2241. Check and comparison signals were finally obtained usually by combining the fluxes from more than one star, as described in the captions to Figures 2 and 3.

Check−Comparison magnitudes showed negligible systematic variation as a function of seeing. However system-

Figure 4. Typical WD fits to the light curves of HV 1620 (left) and HV 2241 (right). Plotted are the $Variable - Comparison$ ($V - Cp$) differential light curve observations, model light curves (lines), $Check - Comparison$ ($Ck - Cp$) and the residuals between Observations and model Computations ($O - C$) for each bandpass ($uvbyVI_{\rm C}$). To facilitate direct comparison, the vertical plot scales are the same for all the light curve plots. Also shown are the spectroscopic radial-velocity curves near quadratures (Niemela & Bassino 1994) (RV – squares for primary component and triangles for secondary component) and residuals to the fit. The units of the RVs are $\mathrm{km\,s^{-1}}$. The rms scatters of the radial velocity residuals are 51 and 39 $\mathrm{km\,s^{-1}}$ for primary and secondary curves respectively for HV 1620 and 29 and 32 $\mathrm{km\,s^{-1}}$ for primary and secondary curves respectively for HV 2241. Rms scatters for the light curves are given in Table 3.

PRINTER: Figure 4 (light curves) go here on a landscape page.

Table 3. Typical exposure durations, signal levels and precisions achieved for the differential photometry.

	u	v	b	y	V	I_C
TYPICAL EXPOSURE TIMES (in seconds)						
	1200	1200	1200	700	400	200
SIGNAL LEVELS†						
HV 1620						
Variable§	−11.2	−10.5	−11.1	−11.5	−12.4	−11.5
Comp$^{(8+12)}$	−12.0	−13.1	−13.8	−14.3		−14.5
Comp$^{(8)}$					−13.3	
Check$^{(3+13)}$	−11.5	−11.9	−13.1	−13.9		−14.7
Check$^{(3)}$					−13.3	
HV 2241						
Variable§	−12.0	−11.8	−12.3	−12.5	−12.7	−12.5
Comp$^{(10)}$	−11.7	−11.5	−12.0	−10.6	−12.5	−12.1
Check$^{(11+13)}$	−11.8	−11.6	−12.1	−12.3	−12.7	−12.1
R.M.S. PRECISIONS (in magnitudes)						
HV 1620						
Var-Comp‡	0.018	0.018	0.017	0.015	0.012	0.017
Check-Comp	0.008	0.009	0.006	0.005	0.005	0.005
HV 2241						
Var-Comp‡	0.016	0.016	0.015	0.012	0.007	0.017
Check-Comp	0.008	0.009	0.011	0.009	0.002	0.011

†Reported in instrumental magnitudes $= -2.5\log_{10}$(ADU above background).
§ Outside eclipse.
‡ With respect to Wilson & Devinney code solutions.

atic effects were seen as a function of seeing in some residuals between light-curve fits and the $Variable - Comparison$ differential photometry. As a result of this, for HV 1620 observations in b, y, V and I_C with FWHM seeing greater than $5''.0$ were eliminated; and a 1 per cent linear correction was applied to the I_C photometry of HV 2241.

Differential magnitudes for the target stars are reported in Tables 1 and 2 and plotted in Figure 4. $Check - Comparison$ magnitudes are also presented in Figure 4. Table 3 reports numerical values for the precision of the $Variable - Comparison$ and $Check - Comparison$ differential photometry.

2.1.2 Photometric calibration

Calibration observations were made on 5 nights for VI_C and on 5 nights for *uvby*. The primary standards for these photometric systems are too bright to observe with a 1-metre telescope. We therefore chose O, B and A-type stars from the following papers for use as secondary standards. For VI_C, stars were taken from Graham (1982), Kilkenny & Menzies (1989), Menzies et al. (1989), Menzies, Marang & Westerhuys (1990) and Landolt (1992) (transformed by Bessell 1995). For *uvby*, stars were chosen from Bessell & Wickramasinghe (1978), Cousins (1987), Graham (1972), Graham & Slettebak (1973), Kilkenny (1977), Kilkenny & Hill (1975), Kilkenny, Hill & Brown (1977) and Kilkenny & Laing (1992). On any particular night, one reference position of the CCD was adopted and all observations were made with the standards and programme stars positioned there. To cancel linear drifts, each object was normally observed multiply in a symmetrical pattern such as VI_CI_CV or *uvbyybvu*, except for Strömgren observations of the eclipsing binaries for which this procedure would have been too time consuming. On each night standards of a range of colours were observed over a range of airmasses.

DAOPHOT was used to extract instrumental fluxes for the standard stars by simple summation over a circular aperture of radius 24 arcsec and correction by a sky signal determined from a larger, concentric annulus. A PSF was determined for each eclipsing binary image. All stars in the vicinity of the target were then subtracted from the image using this PSF and an instrumental flux was determined by aperture integration in the same way as for the standard stars.

Transformation and extinction coefficients were determined from instrumental magnitudes using the simultaneous approach outlined by Harris, Fitzgerald & Reed (1981). Experimentation showed that the final photometry was not sensitive to various reasonable choices for the coefficients. Finally, for simplicity, the same transformation and extinction coefficients were used for all nights with only the zero-points adjusted. For the $(V - I_C)$ colour index there was negligible difference ($\leq$0.001 mag) between values obtained by subtraction of V and I_C reduced independently, and through transformation of the instrumental $(V - I_C)$ values. The Strömgren photometry was reduced to V, $(b - y)$, $(u - b)$ and $(v - b)$: m_1 and c_1 indices were calculated therefrom.

The achieved r.m.s. residuals for the standards stars in magnitudes are for the VI_C photometry: V: 0.012, I_C: 0.031, $(V - I_C)$: 0.033 (161 observations of 19 different standard stars over 5 nights); and for the Strömgren photometry: V: 0.019, $(b-y)$: 0.008, $(u-b)$: 0.014, $(v-b)$: 0.009, m_1: 0.011, c_1: 0.013 (110 observations of 26 different standard stars over 5 nights).

Tables 4 and 5 report the programme star absolute photometry corrected to the phase of the corresponding *IUE* spectrophotometry (see below). The uncertainty in this photometry is undoubtedly dominated by the difficulty of extracting correct instrumental magnitudes for the programme stars. To illustrate this fact, the individual measures are also given in Tables 4 and 5. Results are also given for HV 982, which will be the subject of the next paper in this series. The subtraction of nearby field stars was considerably more difficult for this additional eclipsing binary in the LMC, and the internal agreement of its photometry is considerably worse (e.g. compare the values of V derived from measurements with the V and y filters). We caution that the absolute photometry for HV 1620 and HV 2241 may be more uncertain than indicated by its internal agreement and transformation errors.

Finally, we have compared our mean V photometry with values inferred from Davidge's (1987, 1988) differential light curves and comparison star photometry. Our values are ~0.03 and ~0.06 mag brighter for HV 1620 and HV 2241 respectively. We note that these differences could well be due to bandwidth effects made manifest by the significant colour differences between HV 1620 and HV 2241 and Davidge's comparison stars.

Table 1. HV 1620 differential photometry. Throughout this paper and in earlier ones in the series, mean Heliocentric Julian Dates of observation have been calculated on the basis of UTC, which contains leap-second discontinuities, rather than Terrestrial Time (TT). See e.g. The Hipparcos Catalogue (ESA 1997) for a discussion of the ∼1-minute difference between these two time scales. The columns are Heliocentric Julian Day number, $Variable - Comparison$ magnitude ($V - Cp$), Airmass (X) and FWHM seeing in arcsec (σ).

HJD −2400000	$V-Cp$	X	σ	HJD −2400000	$V-Cp$	X	σ	HJD −2400000	$V-Cp$	X	σ	HJD −2400000	$V-Cp$	X	σ	HJD −2400000	$V-Cp$	X	σ
									u										
49130.8894	0.833	2.22	2.6	49405.9073	0.922	1.57	5.9	49448.9408	1.018	2.10	3.4	49516.1202	1.355	1.42	3.3	49590.2340	0.905	1.19	3.2
49195.8711	0.848	1.85	5.3	49407.0738	0.936	2.15	4.3	49448.9985	1.069	2.22	4.4	49516.1740	1.425	1.29	3.6	49595.8183	1.182	1.69	3.0
49195.9693	0.814	1.50	4.8	49423.9338	0.958	1.84	3.3	49449.0752	1.117	2.16	8.0	49516.2223	1.410	1.22	4.0	49596.0772	1.257	1.15	4.5
49218.9479	1.228	1.38	3.8	49424.1608	0.881	2.12	3.8	49488.8640	1.053	2.18	5.6	49516.2643	1.331	1.17	4.1	49596.1096	1.181	1.14	4.0
49220.1325	0.833	1.14	3.8	49428.9493	1.081	1.95	6.6	49488.9007	1.090	2.22	4.7	49564.0160	0.813	1.35	3.0	49596.1451	1.101	1.14	4.0
49245.8864	1.007	1.35	6.3	49429.0333	1.255	2.19	5.0	49488.9345	1.114	2.22	4.8	49564.2523	0.769	1.15	3.1	49596.1721	1.044	1.15	4.3
49245.9109	1.048	1.30	6.7	49432.9413	1.168	1.96	3.2	49488.9675	1.133	2.16	4.7	49564.2739	0.774	1.16	3.2	49596.2051	0.982	1.18	3.4
49245.9347	1.099	1.26	6.3	49432.9948	1.035	2.13	3.4	49489.0016	1.145	2.08	4.9	49564.8152	0.918	2.01	3.8	49820.0719	0.836	2.14	3.7
49245.9584	1.092	1.22	5.0	49433.0195	1.005	2.19	4.0	49489.0349	1.124	1.96	3.8	49564.8638	0.931	1.83	3.5	49820.1293	0.830	1.96	3.6
49245.9822	1.133	1.19	5.2	49433.0616	0.936	2.23	5.1	49489.0643	1.114	1.85	3.9	49564.9155	0.889	1.64	3.7	49820.1875	0.842	1.74	3.1
49246.0074	1.141	1.17	5.0	49433.1132	0.912	2.18	4.4	49489.1058	1.058	1.70	4.1	49565.8060	0.834	2.04	5.2	49846.2074	1.418	1.44	5.0
49246.0316	1.132	1.15	5.2	49433.1680	0.912	2.03	4.1	49489.1986	0.975	1.40	4.4	49565.8298	0.821	1.95	4.7	49846.2470	1.371	1.34	4.5
49246.0651	1.131	1.14	4.8	49433.2145	0.899	1.86	4.4	49514.1389	0.948	1.38	4.0	49589.8245	0.828	1.73	4.3	49848.0451	1.137	1.99	3.9
49246.0908	1.101	1.14	4.9	49435.8933	0.883	1.81	4.0	49515.8014	0.959	2.19	5.3	49589.8720	0.819	1.56	3.5	49848.0849	1.096	1.84	4.2
49246.1347	1.058	1.16	4.4	49435.9168	0.900	1.90	4.0	49515.8853	0.943	2.18	5.2	49589.9194	0.819	1.42	4.4	49848.1296	1.050	1.67	4.4
49246.1623	1.030	1.18	4.4	49435.9660	0.912	2.07	4.5	49515.9325	0.997	2.06	4.9	49590.0392	0.840	1.19	3.5	49848.1631	1.012	1.56	3.7
49246.1862	1.007	1.20	4.0	49436.0155	0.950	2.19	4.7	49515.9748	1.062	1.92	5.0	49590.0895	0.857	1.15	3.1				
49246.2255	0.982	1.26	3.1	49436.0578	0.962	2.23	5.3	49516.0252	1.146	1.73	4.3	49590.1482	0.864	1.14	3.2				
49372.0365	0.807	1.70	7.0	49448.9147	0.998	2.02	3.3	49516.0776	1.259	1.54	3.7	49590.1943	0.887	1.16	3.3				
									v										
49059.0290	2.767	2.16	3.5	49428.9681	2.799	2.02	5.4	49489.0901	2.791	1.76	4.4	49590.0637	2.576	1.17	3.0	49820.2134	2.566	1.64	3.0
49130.9051	2.545	2.22	2.8	49432.9168	2.897	1.87	2.6	49514.1619	2.677	1.33	4.3	49590.2109	2.619	1.17	3.3	49846.2224	3.065	1.40	4.0
49195.9845	2.504	1.46	4.0	49433.0874	2.605	2.21	3.6	49515.8611	2.637	2.22	4.8	49595.8338	2.887	1.63	3.2	49847.9398	2.759	2.22	4.7
49372.0536	2.494	1.76	6.4	49435.9418	2.587	1.99	4.6	49516.0013	2.781	1.82	4.6	49596.0918	2.912	1.14	4.3	49847.9569	2.813	2.21	4.4
49405.9477	2.581	1.71	5.5	49436.0823	2.648	2.21	5.5	49516.1443	3.062	1.36	3.4	49596.1868	2.715	1.16	3.6	49847.9963	2.822	2.14	5.0
49407.0921	2.621	2.19	3.5	49448.9739	2.748	2.18	3.6	49564.0306	2.520	1.32	2.9	49596.2515	2.630	1.24	3.9	49848.0606	2.812	1.93	4.3
49424.1270	2.594	2.19	3.5	49488.8824	2.753	2.21	4.9	49564.8387	2.626	1.93	3.7	49820.0875	2.528	2.09	3.0				
49424.1761	2.587	2.08	3.4	49488.9861	2.810	2.12	4.5	49589.8482	2.529	1.64	3.6	49820.1454	2.535	1.89	2.9				
									b										
49057.0644	2.757	2.21	3.3	49424.2070	2.715	1.97	3.5	49516.0494	3.019	1.64	3.6	49595.8488	3.065	1.58	3.6	49846.2617	3.143	1.31	3.9
49057.0828	2.746	2.23	3.5	49432.9708	2.936	2.06	2.9	49516.1985	3.245	1.25	3.4	49596.1243	2.985	1.14	3.9	49847.9718	2.971	2.19	3.9
49059.0759	2.922	2.23	3.4	49435.9918	2.745	2.14	4.0	49564.0457	2.681	1.29	2.7	49596.2217	2.841	1.20	3.2	49848.0112	2.975	2.10	4.0
49130.9204	2.700	2.21	2.7	49449.0250	2.961	2.23	4.4	49564.8912	2.806	1.73	3.0	49596.2666	2.739	1.26	3.5	49848.0998	2.954	1.78	3.6
49195.9499	2.660	1.56	4.4	49488.9193	2.972	2.22	4.2	49589.8960	2.684	1.48	3.6	49820.1022	2.680	2.05	2.9				
49195.9999	2.660	1.41	4.1	49489.0200	2.990	2.02	4.4	49590.1146	2.738	1.14	3.1	49820.1601	2.707	1.84	2.8				
49424.1443	2.749	2.16	3.4	49515.9089	2.811	2.13	4.5	49590.2488	2.793	1.21	3.2	49820.2281	2.744	1.59	3.2				
									y										
49057.0934	2.860	2.23	3.6	49424.2202	2.842	1.93	3.6	49489.1823	2.957	1.45	4.6	49590.2607	2.907	1.22	3.0	49820.2011	2.832	1.69	2.5
49059.0931	3.120	2.23	2.6	49433.0407	2.936	2.21	2.9	49515.9539	2.975	2.00	4.5	49595.8611	3.196	1.54	3.4	49820.2442	2.867	1.54	2.9
49130.8764	2.810	2.22	2.3	49433.1889	2.898	1.95	3.7	49516.0984	3.243	1.48	3.1	49596.1571	3.044	1.14	3.9				
49130.9775	2.835	2.09	2.8	49436.0370	2.880	2.22	4.3	49516.2435	3.296	1.19	3.4	49596.2384	2.950	1.22	3.2				
49238.1117	2.809	1.14	2.0	49488.9555	3.095	2.19	4.6	49564.0574	2.812	1.27	2.7	49820.1142	2.811	2.01	2.8				
49424.1908	2.868	2.03	3.5	49489.0521	3.114	1.90	3.7	49590.1698	2.883	1.14	3.1	49820.1721	2.834	1.80	2.7				
									V										
48930.9747	1.052	1.14	3.2	48932.0277	1.097	1.18	3.5	49037.1082	1.081	2.20	2.9	49075.0806	1.034	2.21	3.7	49093.0472	0.989	2.17	3.4
48930.9888	1.031	1.15	3.3	48932.0400	1.092	1.20	4.4	49037.1139	1.078	2.21	2.8	49075.0821	1.040	2.20	3.4	49094.8501	1.018	1.89	3.5
48931.0027	1.028	1.16	3.1	48932.0459	1.104	1.20	4.3	49037.1506	1.096	2.23	2.7	49075.0837	1.045	2.20	3.7	49094.8574	1.002	1.92	3.4
48931.0092	1.027	1.16	3.3	48932.0518	1.104	1.21	4.1	49037.1594	1.102	2.23	2.5	49075.0852	1.038	2.20	3.6	49094.8632	1.001	1.94	3.9
48931.0167	1.021	1.17	4.5	48932.0588	1.098	1.22	4.4	49037.1809	1.102	2.21	2.7	49075.0889	1.041	2.19	3.8	49094.8692	0.991	1.96	4.6
48931.0267	1.020	1.18	3.8	48932.0758	1.139	1.25	3.0	49037.1867	1.110	2.20	3.1	49075.0905	1.039	2.19	3.6	49094.8753	1.010	1.98	4.8
48931.0390	1.016	1.19	3.9	48932.0840	1.144	1.26	2.8	49037.1922	1.103	2.19	3.0	49075.0920	1.034	2.19	3.9	49094.8808	1.005	2.00	4.8
48931.0473	1.017	1.20	3.5	48932.0896	1.152	1.27	2.8	49057.0201	1.031	2.12	3.1	49075.0936	1.034	2.18	4.0	49094.8868	1.005	2.02	4.3
48931.0552	1.013	1.21	3.3	48932.0958	1.157	1.28	2.8	49057.0308	1.035	2.15	3.1	49075.0988	1.022	2.17	3.9	49094.8930	1.008	2.04	4.7
48931.0631	1.011	1.22	3.2	48932.1018	1.161	1.29	2.8	49057.0742	1.043	2.22	4.3	49075.1004	1.043	2.17	4.0	49094.8993	1.029	2.06	4.2
48931.0770	0.995	1.24	3.7	48932.1079	1.162	1.30	2.9	49057.1103	1.060	2.22	4.8	49075.1019	1.047	2.17	3.7	49095.0155	1.035	2.21	4.9
48931.0839	1.008	1.25	3.2	48932.1139	1.172	1.32	2.7	49057.1267	1.048	2.21	4.1	49075.1089	1.028	2.15	3.9	49095.0212	1.035	2.21	4.7
48931.0911	1.004	1.27	3.3	48932.1201	1.180	1.33	2.9	49057.1404	1.075	2.19	3.9	49075.1151	1.031	2.13	3.8	49095.0272	1.051	2.20	4.4
48931.0987	0.995	1.28	3.2	48932.1262	1.191	1.34	2.9	49058.9036	1.094	1.73	2.6	49075.1212	1.031	2.12	3.7	49095.0367	1.059	2.18	4.3
48931.0987	0.995	1.28	3.2	48932.1320	1.203	1.36	2.9	49058.9229	1.092	1.80	3.0	49075.2218	1.066	1.76	3.1	49095.8298	1.069	1.82	4.4
48931.0987	0.995	1.28	3.2	48932.1379	1.209	1.37	3.3	49058.9307	1.093	1.83	2.8	49075.2296	1.065	1.73	3.1	49095.8413	1.049	1.87	4.6
48931.1151	0.991	1.31	3.5	48932.1462	1.221	1.39	3.0	49058.9874	1.125	2.04	2.5	49075.2359	1.066	1.71	3.4	49095.8472	1.068	1.89	4.0
48931.1257	0.992	1.34	3.8	48932.1530	1.227	1.41	3.9	49059.0376	1.184	2.18	2.9	49075.2419	1.063	1.69	3.4	49095.8534	1.062	1.91	4.1
48931.1325	0.992	1.35	3.7	48932.1593	1.236	1.42	4.0	49059.0549	1.193	2.21	2.6	49092.0424	1.305	2.19	3.8	49095.8592	1.058	1.93	4.1
48931.1395	0.997	1.37	4.2	48932.1654	1.255	1.44	3.6	49059.0647	1.214	2.22	2.7	49092.0504	1.287	2.17	4.1	49095.8651	1.059	1.96	4.0
48931.1464	0.988	1.38	4.4	48932.1713	1.258	1.46	3.3	49059.1195	1.305	2.21	2.7	49092.0564	1.275	2.16	3.9	49095.8710	1.059	1.98	3.6
48931.1539	0.989	1.40	4.4	48932.1774	1.265	1.48	3.3	49059.1296	1.326	2.20	2.5	49092.0626	1.264	2.15	3.5	49095.8767	1.056	2.00	4.1
48931.1599	0.982	1.42	4.2	48954.9288	0.963	1.15	3.7	49059.1368	1.336	2.18	2.6	49092.0695	1.241	2.13	3.4	49095.8822	1.056	2.02	3.6
48931.1672	0.985	1.44	3.8	48954.9545	0.957	1.17	4.1	49059.1422	1.344	2.17	3.1	49092.0764	1.230	2.11	3.8	49095.8881	1.053	2.04	3.7
48931.1757	0.978	1.46	3.9	48954.9734	0.962	1.19	3.5	49059.1482	1.355	2.16	2.5	49092.0822	1.229	2.09	3.7	49095.9788	1.035	2.22	4.1
48931.9114	1.071	1.14	2.7	48955.0029	0.956	1.23	3.3	49059.1539	1.364	2.14	2.9	49092.0902	1.217	2.07	3.5	49095.9886	1.032	2.23	4.0
48931.9181	1.072	1.14	2.8	48955.0343	0.976	1.28	3.5	49059.1605	1.384	2.13	3.2	49092.0958	1.207	2.05	3.3	49095.9954	1.030	2.22	4.5
48931.9239	1.073	1.14	3.1	48955.1378	0.966	1.55	3.6	49059.1669	1.391	2.11	2.8	49092.1016	1.187	2.03	3.4	49099.0086	1.293	2.21	4.5
48931.9332	1.080	1.14	2.6	48955.1449	0.961	1.57	4.1	49059.1751	1.416	2.09	2.8	49092.8619	0.971	1.91	2.5	49099.0254	1.317	2.18	4.4
48931.9399	1.076	1.14	2.7	49017.9988	1.065	1.67	4.2	49059.1809	1.424	2.07	2.6	49092.8697	0.971	1.94	2.8	49099.0408	1.352	2.15	4.9
48931.9470	1.077	1.14	2.8	49018.0211	1.059	1.75	4.0	49059.1870	1.442	2.05	2.6	49092.8828	0.982	1.99	3.1	49130.9963	0.985	2.04	3.1
48931.9531	1.082	1.14	2.9	49018.0530	1.045	1.87	4.5	49059.1940	1.427	2.02	2.1	49092.8908	0.974	2.02	2.7	49131.0017	0.988	2.02	2.9
48931.9734	1.082	1.14	2.8	49036.9014	1.024	1.51	3.0	49059.2002	1.463	2.00	2.8	49092.8970	0.979	2.04	3.0	49131.0085	0.983	1.99	3.0
48931.9797	1.086	1.15	2.8	49036.9198	1.027	1.58	2.9	49075.0467	1.012	2.23	3.2	49092.9070	0.978	2.07	3.0	49131.0142	0.983	1.97	2.7
48931.9870	1.080	1.15	3.3	49036.9385	1.029	1.64	3.4	49075.0578	1.014	2.23	3.1	49092.9131	0.967	2.09	3.1	49131.0197	0.986	1.95	3.0
48931.9946	1.089	1.15	3.4	49036.9816	1.050	1.80	4.1	49075.0644	1.016	2.22	3.0	49092.9190	0.978	2.11	3.0	49131.2624	1.044	1.24	3.0
48932.0009	1.084	1.16	3.4	49037.0270	1.062	1.97	3.1	49075.0721	1.036	2.22	3.6	49092.9246	0.973	2.12	2.9	49131.2685	1.049	1.23	2.8
48932.0078	1.089	1.16	3.6	49037.0475	1.066	2.04	3.9	49075.0736	1.034	2.21	3.7	49092.9319	0.969	2.14	3.0	49131.2740	1.043	1.22	3.0
48932.0144	1.089	1.17	3.6	49037.0653	1.074	2.10	3.0	49075.0752	1.024	2.21	4.0	49093.0329	0.980	2.20	3.5	49131.2794	1.045	1.21	3.1
48932.0209	1.096	1.18	3.5	49037.0880	1.075	2.16	2.8	49075.0767	1.044	2.21	3.5	49093.0413	0.986	2.19	3.3	49131.2848	1.046	1.21	2.9

continued on next page.

Table 1. (cont).

HJD −2400000	$V-Cp$	X	σ	HJD −2400000	$V-Cp$	X	σ	HJD −2400000	$V-Cp$	X	σ	HJD −2400000	$V-Cp$	X	σ	HJD −2400000	$V-Cp$	X	σ
									V										
49131.2907	1.045	1.20	3.1	49237.0341	1.426	1.17	2.6	49246.0177	1.291	1.16	4.1	49436.0476	1.063	2.22	4.6	49516.2327	1.474	1.20	3.2
49195.2054	1.262	1.14	4.9	49237.0415	1.418	1.16	2.5	49246.0482	1.290	1.14	4.1	49436.0721	1.060	2.22	4.9	49516.2507	1.450	1.18	3.2
49195.2292	1.283	1.14	4.9	49237.0505	1.397	1.15	2.5	49246.0759	1.270	1.14	4.0	49448.8967	1.123	1.95	2.6	49564.0013	0.982	1.39	2.7
49195.2429	1.274	1.14	5.0	49237.0564	1.390	1.15	3.0	49246.1210	1.229	1.15	3.3	49448.9260	1.155	2.05	2.3	49564.2272	0.943	1.14	2.7
49195.2737	1.289	1.15	4.4	49237.0662	1.365	1.15	2.8	49246.1468	1.209	1.16	3.3	49448.9552	1.182	2.14	2.7	49564.2393	0.945	1.14	2.4
49195.2799	1.284	1.16	4.7	49237.0722	1.354	1.14	2.9	49246.1725	1.181	1.19	3.3	49448.9880	1.203	2.20	3.4	49564.2618	0.947	1.15	2.4
49195.8383	0.982	1.97	4.6	49237.0804	1.339	1.14	2.5	49246.2057	1.149	1.23	3.7	49449.0353	1.245	2.22	4.2	49564.2834	0.943	1.17	2.5
49195.8544	0.975	1.91	4.3	49237.0876	1.327	1.14	2.6	49246.2358	1.145	1.28	2.6	49488.8498	1.164	2.14	4.9	49564.8021	1.050	2.06	3.7
49195.8932	0.974	1.77	4.0	49237.0932	1.309	1.14	2.8	49423.9029	1.154	1.72	2.5	49489.0797	1.241	1.80	4.1	49564.8252	1.060	1.98	3.2
49195.9224	0.972	1.66	4.5	49237.0997	1.297	1.14	2.6	49423.9090	1.146	1.74	2.3	49489.1195	1.193	1.65	4.4	49564.8487	1.064	1.90	2.9
49195.9347	0.963	1.62	4.2	49237.1069	1.290	1.14	2.7	49426.9592	1.040	1.96	4.7	49489.1749	1.144	1.47	4.3	49564.8777	1.081	1.79	2.6
49218.9374	1.369	1.42	3.4	49237.1127	1.271	1.14	2.8	49432.8797	1.379	1.73	2.3	49489.2123	1.106	1.37	4.2	49564.9013	1.088	1.70	2.6
49218.9746	1.289	1.33	3.5	49237.1189	1.261	1.14	2.4	49432.9064	1.326	1.83	2.6	49514.1259	1.104	1.42	3.3	49565.7909	0.972	2.09	4.8
49218.9937	1.250	1.29	3.7	49237.1250	1.253	1.14	2.6	49432.9310	1.277	1.92	2.4	49514.1489	1.116	1.36	3.2	49565.8399	0.983	1.92	4.6
49220.1220	1.028	1.14	2.8	49237.1323	1.239	1.14	2.8	49432.9604	1.222	2.02	2.6	49514.1719	1.142	1.31	3.1	49565.8642	0.974	1.83	4.4
49236.9023	1.479	1.38	3.4	49237.1427	1.213	1.15	2.8	49432.9842	1.182	2.10	2.6	49515.7880	1.062	2.17	4.6	49589.8081	0.964	1.79	3.7
49236.9175	1.498	1.34	3.5	49237.1488	1.202	1.15	2.8	49433.0088	1.139	2.16	2.5	49515.8478	1.083	2.23	4.4	49589.8348	0.971	1.69	3.7
49236.9235	1.501	1.33	3.2	49237.1547	1.191	1.15	2.6	49433.0334	1.112	2.20	3.2	49515.8717	1.087	2.21	4.5	49589.8583	0.977	1.61	3.0
49236.9318	1.511	1.31	3.1	49237.1605	1.182	1.15	2.7	49433.0511	1.101	2.22	2.7	49515.8956	1.089	2.17	4.5	49589.8822	0.977	1.53	3.0
49236.9376	1.510	1.30	3.1	49237.1662	1.169	1.16	2.9	49433.0770	1.080	2.22	3.0	49515.9191	1.112	2.11	4.0	49589.9061	0.979	1.46	3.4
49236.9461	1.521	1.28	2.9	49237.1729	1.162	1.16	2.8	49433.1015	1.064	2.20	3.4	49515.9433	1.140	2.03	4.1	49590.0249	1.013	1.21	3.2
49236.9518	1.513	1.27	2.7	49237.1785	1.155	1.17	2.8	49433.1268	1.047	2.15	3.7	49515.9612	1.161	1.97	4.1	49590.0498	1.016	1.18	3.1
49236.9589	1.515	1.26	3.0	49237.1840	1.143	1.17	2.5	49433.1567	1.056	2.07	4.2	49515.9855	1.187	1.88	4.4	49590.0740	1.029	1.16	3.0
49236.9651	1.514	1.25	2.9	49237.1924	1.128	1.18	2.7	49433.1815	1.055	1.98	4.1	49516.0117	1.228	1.78	3.9	49590.0997	1.027	1.15	3.0
49236.9716	1.510	1.24	2.5	49237.1980	1.121	1.19	2.7	49433.2034	1.047	1.90	4.0	49516.0355	1.280	1.70	3.5	49590.1276	1.040	1.14	2.6
49236.9793	1.503	1.23	2.5	49237.2270	1.095	1.22	2.8	49435.8759	1.032	1.74	3.5	49516.0631	1.328	1.60	3.2	49590.1583	1.042	1.14	3.1
49236.9871	1.504	1.22	2.8	49237.2331	1.090	1.23	2.8	49435.9034	1.035	1.85	3.2	49516.0877	1.372	1.52	2.9	49590.1769	1.044	1.15	2.9
49236.9948	1.489	1.21	2.5	49237.2388	1.079	1.24	2.8	49435.9272	1.040	1.93	3.7	49516.1057	1.412	1.46	2.8	49590.2208	1.058	1.18	3.2
49237.0060	1.482	1.19	2.6	49245.8975	1.195	1.33	4.8	49435.9520	1.051	2.02	3.9	49516.1306	1.447	1.39	2.6	49590.2677	1.067	1.23	3.2
49237.0151	1.469	1.18	2.8	49245.9450	1.244	1.24	4.8	49435.9778	1.050	2.10	3.3	49516.1559	1.486	1.34	2.9	49760.9066	1.248	1.48	2.6
49237.0221	1.450	1.18	2.6	49245.9686	1.273	1.21	4.4	49436.0022	1.062	2.16	3.7	49516.1846	1.499	1.28	3.1	49760.9218	1.258	1.52	2.9
49237.0278	1.448	1.17	2.7	49245.9923	1.289	1.18	4.0	49436.0259	1.061	2.21	4.1	49516.2087	1.493	1.24	3.1				
									I_C										
49057.1003	3.174	2.23	3.6	49246.0816	3.365	1.14	3.9	49435.9828	3.171	2.12	3.4	49515.9236	3.233	2.10	4.3	49589.8629	3.087	1.60	2.8
49059.1011	3.385	2.23	2.7	49246.1257	3.337	1.15	3.3	49436.0065	3.189	2.17	3.7	49515.9477	3.261	2.02	4.0	49589.8867	3.108	1.52	3.1
49130.9383	3.062	2.19	2.7	49246.1532	3.323	1.17	3.6	49436.0303	3.166	2.21	3.8	49515.9655	3.273	1.96	3.8	49589.9105	3.109	1.45	3.9
49130.9519	3.081	2.16	2.0	49246.1770	3.299	1.19	3.6	49436.0432	3.179	2.22	4.1	49515.9923	3.305	1.86	4.2	49590.0299	3.125	1.21	2.7
49130.9570	3.097	2.15	2.2	49246.2163	3.280	1.24	2.7	49436.0671	3.182	2.22	5.0	49516.0162	3.341	1.77	3.9	49590.0545	3.126	1.18	2.8
49130.9611	3.128	2.14	2.4	49246.2405	3.227	1.28	2.7	49448.9029	3.248	1.97	2.6	49516.0402	3.379	1.68	3.1	49590.0803	3.129	1.16	2.5
49195.1934	3.357	1.14	4.5	49423.9145	3.251	1.76	2.7	49448.9505	3.287	2.12	2.9	49516.0685	3.418	1.58	2.9	49590.1047	3.130	1.14	2.4
49195.2001	3.367	1.14	4.7	49423.9178	3.238	1.78	2.7	49448.9595	3.295	2.15	3.2	49516.0923	3.458	1.50	2.8	49590.1339	3.136	1.14	2.4
49195.2105	3.369	1.14	4.8	49423.9238	3.250	1.80	2.8	49448.9830	3.316	2.19	3.8	49516.1112	3.488	1.45	2.8	49590.1622	3.161	1.14	2.6
49195.2235	3.380	1.14	4.4	49424.2268	3.111	1.91	3.2	49449.0099	3.337	2.22	3.8	49516.1350	3.506	1.38	2.4	49590.1819	3.159	1.15	2.6
49195.2344	3.383	1.14	4.1	49428.9586	3.302	1.98	4.8	49449.0397	3.356	2.22	4.7	49516.1650	3.545	1.32	2.8	49590.2250	3.177	1.18	2.7
49195.2545	3.398	1.14	4.1	49432.8751	3.427	1.71	2.3	49488.8546	3.275	2.15	4.2	49516.1894	3.555	1.27	2.8	49590.2719	3.164	1.24	2.6
49195.2656	3.381	1.15	3.7	49432.8989	3.409	1.80	2.3	49488.8732	3.286	2.19	4.2	49516.2132	3.558	1.23	3.2	49595.8094	3.322	1.73	2.6
49195.8430	3.143	1.96	4.4	49432.9258	3.376	1.90	2.2	49488.9101	3.332	2.23	3.8	49516.2372	3.528	1.20	3.1	49596.0676	3.457	1.15	3.2
49195.8470	3.091	1.94	4.5	49432.9541	3.345	2.00	2.5	49488.9484	3.389	2.20	3.9	49516.2552	3.521	1.18	3.3	49596.1008	3.406	1.14	3.5
49195.8609	3.087	1.89	4.2	49432.9798	3.294	2.09	2.6	49488.9766	3.382	2.15	4.1	49564.0072	3.108	1.38	2.5	49596.1333	3.356	1.14	3.2
49195.8874	3.088	1.79	4.2	49433.0042	3.265	2.15	2.6	49489.0106	3.374	2.05	4.8	49564.2336	3.067	1.14	2.4	49596.1630	3.310	1.15	3.4
49195.8985	3.077	1.75	4.6	49433.0288	3.229	2.20	3.1	49489.0455	3.375	1.93	3.5	49564.2433	3.072	1.14	2.4	49596.1960	3.262	1.17	2.9
49195.9288	3.092	1.64	4.5	49433.0467	3.224	2.22	2.7	49489.0736	3.353	1.83	3.6	49564.2654	3.085	1.15	2.4	49596.2314	3.218	1.20	2.9
49195.9400	3.092	1.60	4.2	49433.0725	3.189	2.22	3.0	49489.1149	3.324	1.67	3.7	49564.2869	3.065	1.17	2.7	49760.9117	3.335	1.49	2.8
49218.9618	3.385	1.36	3.1	49433.0967	3.187	2.21	3.5	49489.1704	3.257	1.49	4.2	49564.8063	3.156	2.05	3.3	49760.9167	3.345	1.51	3.0
49219.0116	3.309	1.26	3.3	49433.1223	3.176	2.16	3.4	49489.2080	3.237	1.38	3.5	49564.8297	3.160	1.97	3.4	49820.0615	3.048	2.17	2.5
49220.1429	3.121	1.14	2.6	49433.1523	3.177	2.08	3.4	49514.1301	3.211	1.41	3.2	49564.8532	3.170	1.88	2.7	49820.1202	3.081	1.99	2.5
49245.9019	3.298	1.32	4.8	49433.1771	3.175	2.00	3.5	49514.1530	3.226	1.36	3.8	49564.8821	3.172	1.77	2.5	49820.1781	3.092	1.78	2.4
49245.9493	3.386	1.24	4.3	49433.1954	3.178	1.93	3.5	49514.1820	3.275	1.29	3.0	49564.9063	3.211	1.68	2.7	49820.2379	3.131	1.57	3.2
49245.9731	3.367	1.20	4.5	49435.8827	3.165	1.77	3.1	49515.7924	3.172	2.18	4.2	49565.7971	3.104	2.07	4.0				
49245.9969	3.398	1.18	4.4	49435.9079	3.163	1.86	2.8	49515.8521	3.180	2.22	4.0	49565.8441	3.102	1.91	3.9				
49246.0221	3.396	1.16	4.9	49435.9317	3.173	1.95	3.5	49515.8762	3.193	2.20	4.3	49589.8152	3.083	1.77	3.4				
49246.0551	3.395	1.14	3.7	49435.9569	3.167	2.04	3.6	49515.8999	3.209	2.16	3.8	49589.8392	3.086	1.68	3.2				

2.1.3 Flux calibration

We shall need to convert our standard-system photometry into extra-atmospheric fluxes for effective temperature determinations. Bessell (1979) has already published a flux calibration for Cousins photometry, while Underhill (1981) and Heber et al. (1984) have published calibrations for *uvby* photometry.

We have calculated new calibrations because improved model atmospheres are now available for Vega (Castelli & Kurucz 1994). The procedure of Heber et al. was followed. Bandpass-weighted fluxes for Vega were computed using the Kurucz Vega model with $T_{\rm eff} = 9\,550$ K, $\log g = 3.95$ and $[m/H] = -0.5$ and scaled to match Vega's observed extra-atmospheric flux at 555.6 nm (Mégessier 1995). Photometry of Vega was taken from Crawford et al. (1972) for *uvby* and from Johnson (1965) for $UBVR_{\rm J}I_{\rm J}$ which was subsequently transformed to $R_{\rm C}I_{\rm C}$ via the equations given by Bessell (1979). Our flux calibration is compared with the ones above in Table 6. Mégessier estimates 0.7 per cent as the uncertainty of her Vega flux: our calibration is uncertain at at least this level.

2.2 Ultraviolet spectrophotometry

The *IUE* satellite was used from the Goddard groundstation to acquire low-resolution uv spectra with the SWP camera and large entrance aperture, as detailed in Table 7. The spectra were reprocessed with the Final Archive (NEWSIPS) software in order to obtain improved spectral resolution and to correct for the variation of the camera sensitivity with temperature and time (e.g. Garhart 1992; Nichols & Linsky 1996). The uncertainty in the reprocessed fluxes is estimated to be ∼5 per cent (Imhoff, priv. comm.).

Table 2. HV 2241 differential photometry. Columns as for Table 1.

HJD −2400000	$V-Cp$	X	σ	HJD −2400000	$V-Cp$	X	σ	HJD −2400000	$V-Cp$	X	σ	HJD −2400000	$V-Cp$	X	σ	HJD −2400000	$V-Cp$	X	σ
									u										
49172.0992	−0.188	2.12	3.1	49451.8291	0.334	1.23	2.8	49626.9571	−0.215	1.55	4.1	49659.0855	−0.278	1.09	6.0	49719.0057	−0.031	1.10	5.7
49172.1194	−0.203	1.99	3.4	49451.8659	0.233	1.33	3.5	49628.9701	−0.216	1.48	3.8	49659.8862	0.164	1.47	4.2	49719.0395	−0.069	1.14	7.9
49172.1339	−0.195	1.90	3.5	49451.9033	0.146	1.45	3.3	49629.1493	−0.152	1.10	3.9	49659.9314	0.274	1.32	4.0	49719.0681	−0.087	1.18	7.0
49427.9321	0.071	1.33	3.8	49451.9357	0.070	1.58	3.6	49630.9437	−0.297	1.56	3.0	49659.9679	0.361	1.23	4.3	49720.9337	0.684	1.08	4.5
49427.9723	0.029	1.46	3.4	49451.9729	−0.004	1.77	4.1	49630.9800	−0.289	1.42	2.9	49660.0080	0.472	1.16	4.4	49720.9720	0.619	1.09	4.1
49431.9219	0.008	1.33	3.5	49452.0148	−0.074	2.01	2.8	49631.0163	−0.296	1.31	2.9	49660.1398	0.666	1.09	5.9	49721.0050	0.534	1.11	5.6
49431.9709	0.041	1.50	3.6	49452.0522	−0.120	2.25	3.3	49631.0484	−0.287	1.23	2.8	49660.1578	0.642	1.10	6.2	49721.0323	0.444	1.13	3.5
49432.0127	0.098	1.69	2.9	49452.1079	−0.155	2.60	3.4	49657.8763	0.155	1.53	4.1	49660.9534	−0.258	1.26	8.0	49721.0652	0.365	1.18	3.8
49432.0488	0.139	1.89	3.4	49452.1464	−0.171	2.76	3.9	49657.9098	0.186	1.41	4.2	49660.9725	−0.286	1.22	8.1	49721.1000	0.260	1.25	4.1
49432.0911	0.169	2.15	4.2	49452.2253	−0.203	2.73	4.3	49657.9432	0.201	1.30	4.3	49661.0055	−0.278	1.16	7.8	49721.1269	0.190	1.32	4.4
49432.1321	0.190	2.42	3.6	49591.9667	−0.313	2.01	3.9	49657.9716	0.200	1.23	4.4	49661.0527	−0.293	1.11	8.4	49760.1318	0.397	1.78	3.7
49432.1722	0.158	2.65	4.2	49599.8323	−0.195	2.70	5.0	49658.0051	0.176	1.17	4.7	49661.0800	−0.291	1.09	8.0	49778.9876	−0.217	1.38	3.1
49432.2197	0.119	2.80	5.0	49599.8655	−0.205	2.52	5.2	49658.0415	0.136	1.12	4.6	49661.1134	−0.287	1.08	7.9	49779.0283	−0.210	1.53	3.4
49449.9247	−0.185	1.51	4.4	49599.9011	−0.227	2.30	3.7	49658.0706	0.097	1.10	5.1	49661.1465	−0.297	1.09	7.6	49779.0666	−0.194	1.71	3.6
49449.9726	−0.196	1.74	5.3	49599.9284	−0.220	2.12	3.7	49658.1058	0.053	1.08	5.0	49715.0570	−0.220	1.14	4.2				
49450.0173	−0.210	1.99	6.7	49599.9639	−0.236	1.89	3.7	49658.1393	0.015	1.09	5.3	49715.0916	−0.218	1.20	4.2				
49450.0732	−0.245	2.36	6.2	49600.0001	−0.237	1.70	3.9	49658.1693	−0.018	1.10	3.1	49715.1256	−0.233	1.27	4.3				
49450.1268	−0.238	2.66	7.3	49600.0278	−0.252	1.57	3.8	49658.8832	−0.287	1.49	5.0	49718.9720	−0.002	1.09	5.2				
									v										
49172.1490	−0.242	1.81	3.0	49449.9513	−0.235	1.63	4.6	49599.8470	−0.239	2.63	5.2	49659.1002	−0.302	1.08	5.2	49721.0472	0.317	1.15	3.5
49172.1660	−0.241	1.72	3.1	49450.0409	−0.267	2.14	5.5	49599.9434	−0.282	2.02	3.4	49659.9084	0.154	1.39	3.9	49760.1501	0.270	1.89	3.6
49172.1814	−0.246	1.64	2.9	49451.8472	0.215	1.28	2.8	49626.9796	−0.260	1.46	4.1	49660.9873	−0.332	1.19	7.1	49779.0031	−0.252	1.43	3.4
49427.9539	0.013	1.40	3.3	49451.9543	−0.012	1.67	3.6	49657.8917	0.152	1.47	3.5	49661.0953	−0.324	1.08	7.2				
49431.9435	−0.006	1.40	3.2	49452.0713	−0.182	2.38	3.3	49657.9865	0.164	1.20	4.0	49715.0725	−0.266	1.17	3.7				
49432.0701	0.131	2.02	4.0	49452.2003	−0.266	2.80	3.3	49658.0854	0.035	1.09	4.4	49718.9870	−0.038	1.09	5.1				
49432.1955	0.106	2.74	4.6	49452.2003	−0.266	2.80	3.3	49658.8981	−0.337	1.44	4.9	49720.9485	0.571	1.08	4.6				
									b										
49172.1960	−0.266	1.58	2.8	49450.0922	−0.274	2.48	5.9	49599.9789	−0.275	1.81	3.4	49659.1152	−0.335	1.08	5.5	49721.0817	0.221	1.21	3.5
49172.2177	−0.271	1.49	2.9	49450.1467	−0.300	2.74	6.3	49629.1642	−0.202	1.09	3.8	49659.9497	0.246	1.27	4.1	49760.1685	0.223	2.00	3.8
49172.2329	−0.287	1.43	3.0	49451.8846	0.115	1.38	3.1	49630.9981	−0.329	1.36	2.7	49661.0336	−0.335	1.12	8.0	49779.0437	−0.239	1.60	3.1
49427.9937	−0.033	1.55	2.7	49451.9948	−0.097	1.89	2.8	49657.9247	0.165	1.36	4.1	49661.1283	−0.338	1.09	7.7				
49431.9916	0.022	1.59	3.4	49452.1268	−0.205	2.69	3.3	49658.0234	0.130	1.14	4.1	49715.1071	−0.279	1.23	3.7				
49432.1116	0.163	2.29	3.6	49452.2446	−0.251	2.65	4.0	49658.1211	0.009	1.08	4.1	49719.0213	−0.077	1.12	6.1				
49449.9938	−0.254	1.85	4.7	49599.8805	−0.245	2.43	4.5	49658.9134	−0.326	1.38	4.5	49720.9869	0.482	1.09	4.5				
									y										
49172.2466	−0.333	1.39	2.9	49450.1108	−0.310	2.58	5.8	49599.9131	−0.319	2.22	3.2	49658.9257	−0.376	1.35	4.0	49719.0521	−0.151	1.15	6.7
49172.2557	−0.341	1.36	2.9	49450.1622	−0.341	2.79	7.6	49600.0122	−0.341	1.64	3.4	49659.1329	−0.356	1.09	5.4	49721.0173	0.330	1.12	3.3
49172.2661	−0.353	1.33	2.5	49451.9202	−0.005	1.51	2.9	49631.0333	−0.372	1.26	2.6	49659.9798	0.265	1.21	3.6	49721.1119	0.100	1.28	3.8
49432.0308	0.046	1.78	3.1	49452.0360	−0.189	2.14	3.1	49657.9553	0.147	1.27	4.0	49661.0646	−0.377	1.10	6.9	49721.1390	0.043	1.36	4.5
49432.1533	0.107	2.54	4.5	49452.1638	−0.258	2.80	3.8	49658.0543	0.053	1.11	4.7	49661.1585	−0.390	1.10	7.3	49760.1837	0.122	2.09	3.9
49450.0563	−0.302	2.24	5.6	49452.2601	−0.317	2.57	3.6	49658.1515	−0.071	1.09	4.8	49715.1383	−0.327	1.30	4.9				
									V										
49753.9786	−0.286	1.18	2.8	49753.9827	−0.289	1.19	2.8	49784.1056	−0.097	2.01	3.9	49784.1209	−0.111	2.11	4.2				
									$\boldsymbol{I}_{\rm C}$										
49172.2728	−0.390	1.31	2.4	49432.2049	0.031	2.77	4.3	49452.2154	−0.323	2.77	3.7	49657.9007	0.096	1.45	3.3	49711.1346	−0.397	1.26	5.2
49172.2761	−0.394	1.30	2.5	49432.2081	0.045	2.78	4.3	49452.2355	−0.353	2.70	3.4	49657.9341	0.114	1.34	3.8	49711.1378	−0.398	1.27	5.3
49172.2792	−0.395	1.29	2.4	49432.2286	−0.008	2.81	4.3	49452.2536	−0.327	2.61	3.5	49657.9625	0.128	1.26	3.7	49711.1410	−0.398	1.28	5.4
49427.9183	−0.016	1.29	2.8	49449.9080	−0.291	1.44	3.3	49591.9568	−0.412	2.09	3.1	49657.9958	0.109	1.19	4.1	49711.1442	−0.384	1.29	5.7
49427.9230	−0.016	1.30	3.1	49449.9139	−0.294	1.46	3.3	49591.9825	−0.396	1.92	3.1	49658.0324	0.071	1.13	3.9	49711.1478	−0.396	1.30	5.9
49427.9414	−0.038	1.35	2.7	49449.9345	−0.298	1.54	4.1	49591.9961	−0.392	1.84	3.3	49658.0608	0.034	1.11	4.1	49711.1510	−0.381	1.31	5.4
49427.9447	−0.040	1.36	2.6	49449.9407	−0.310	1.57	3.9	49592.0063	−0.404	1.78	3.1	49658.0945	−0.022	1.09	4.2	49715.0290	−0.335	1.11	3.5
49427.9630	−0.065	1.42	2.4	49449.9604	−0.319	1.66	3.6	49592.0161	−0.387	1.73	3.3	49658.1302	−0.069	1.08	4.0	49715.0439	−0.334	1.13	3.4
49427.9813	−0.090	1.49	3.2	49449.9636	−0.307	1.68	4.3	49592.1167	−0.376	1.33	2.8	49658.1600	−0.104	1.09	2.6	49715.0819	−0.358	1.18	3.3
49427.9845	−0.091	1.50	2.7	49449.9816	−0.290	1.77	5.5	49592.1336	−0.360	1.28	2.8	49658.1787	−0.111	1.11	2.4	49715.1165	−0.349	1.25	3.6
49428.0031	−0.110	1.58	2.3	49449.9848	−0.316	1.79	4.8	49592.1450	−0.359	1.25	3.2	49658.8742	−0.403	1.54	3.6	49715.1447	−0.353	1.32	4.5
49428.0066	−0.114	1.60	2.5	49450.0028	−0.307	1.89	4.4	49592.1555	−0.360	1.23	3.5	49658.9318	−0.407	1.33	3.9	49718.9623	−0.087	1.08	4.6
49431.9021	−0.120	1.27	2.6	49450.0070	−0.310	1.92	4.5	49592.1613	−0.375	1.22	3.7	49659.0760	−0.398	1.09	5.3	49718.9967	−0.132	1.10	4.5
49431.9053	−0.114	1.28	2.5	49450.0285	−0.318	2.05	5.2	49592.1722	−0.356	1.20	3.4	49659.1591	−0.399	1.10	4.7	49719.0304	−0.160	1.12	6.1
49431.9090	−0.111	1.29	2.5	49450.0316	−0.320	2.07	4.8	49592.1806	−0.349	1.18	3.6	49659.8660	−0.015	1.56	3.0	49719.0591	−0.189	1.16	5.8
49431.9124	−0.110	1.30	2.7	49450.0501	−0.335	2.19	4.4	49592.1863	−0.403	1.17	3.8	49659.8771	0.001	1.52	3.6	49719.0934	−0.193	1.22	7.8
49431.9310	−0.082	1.35	2.6	49450.0629	−0.332	2.28	5.2	49592.2136	−0.382	1.13	4.1	49659.8967	0.031	1.44	3.4	49720.9247	0.458	1.09	3.4
49431.9343	−0.073	1.36	2.7	49450.0829	−0.332	2.41	5.2	49599.8228	−0.293	2.74	3.4	49659.9204	0.082	1.36	3.1	49720.9577	0.424	1.08	4.8
49431.9581	−0.081	1.44	3.2	49450.1035	−0.341	2.53	5.3	49599.8561	−0.304	2.59	4.4	49659.9407	0.114	1.30	3.6	49720.9959	0.360	1.10	4.8
49431.9617	−0.073	1.46	3.2	49450.1175	−0.341	2.61	5.8	49599.8897	−0.325	2.38	4.6	49659.9587	0.167	1.25	3.6	49721.0233	0.285	1.12	2.9
49431.9797	−0.056	1.53	3.0	49450.1558	−0.377	2.77	5.8	49599.9192	−0.340	2.19	3.0	49659.9989	0.267	1.17	3.5	49721.0562	0.193	1.16	3.0
49431.9827	−0.046	1.54	3.1	49450.1689	−0.362	2.80	6.8	49599.9526	−0.343	1.98	2.9	49660.0541	0.402	1.11	3.9	49721.0907	0.113	1.23	3.6
49432.0007	−0.032	1.62	2.9	49451.8200	0.206	1.21	2.3	49599.9911	−0.345	1.75	3.2	49660.0585	0.386	1.10	3.9	49721.1180	0.055	1.29	3.5
49432.0038	−0.021	1.64	2.8	49451.8382	0.153	1.25	2.4	49600.0183	−0.355	1.62	2.9	49660.1045	0.450	1.08	4.5	49721.1452	0.002	1.37	3.9
49432.0217	−0.001	1.73	2.7	49451.8563	0.114	1.29	2.5	49626.9480	−0.332	1.60	3.4	49660.1083	0.471	1.08	4.5	49753.9534	−0.300	1.15	2.8
49432.0247	0.007	1.74	2.8	49451.8752	0.072	1.35	3.1	49626.9698	−0.328	1.51	3.5	49660.1120	0.462	1.08	4.3	49753.9924	−0.310	1.21	4.2
49432.0368	0.024	1.81	2.8	49451.8937	0.026	1.41	2.8	49626.9904	−0.338	1.43	3.6	49660.1203	0.457	1.08	4.7	49754.1043	−0.329	1.56	4.9
49432.0399	0.032	1.82	3.0	49451.9132	−0.023	1.48	2.6	49628.9552	−0.329	1.54	3.1	49660.1237	0.478	1.08	4.4	49754.1126	−0.332	1.60	5.4
49432.0579	0.054	1.93	3.3	49451.9265	−0.036	1.53	3.0	49628.9610	−0.347	1.52	3.2	49660.1270	0.461	1.08	5.1	49754.1179	−0.333	1.62	4.8
49432.0611	0.058	1.95	3.1	49451.9453	−0.078	1.62	2.9	49629.0350	−0.343	1.28	3.3	49660.1302	0.461	1.08	4.3	49754.1214	−0.337	1.64	4.3
49432.0792	0.078	2.06	3.2	49451.9637	−0.085	1.71	3.4	49629.0388	−0.355	1.27	3.0	49660.1488	0.451	1.09	4.6	49754.1270	−0.342	1.66	4.5
49432.0823	0.071	2.08	3.2	49451.9834	−0.128	1.81	3.8	49629.1344	−0.283	1.11	3.1	49660.1668	0.428	1.10	5.3	49760.1221	0.231	1.72	3.2
49432.0998	0.087	2.20	3.1	49452.0047	−0.171	1.94	2.5	49629.1402	−0.284	1.11	3.2	49660.9416	−0.374	1.29	6.9	49760.1410	0.194	1.82	2.9
49432.1028	0.093	2.21	3.4	49452.0292	−0.204	2.09	2.7	49630.9244	−0.448	1.66	3.2	49660.9633	−0.395	1.24	6.7	49760.1591	0.149	1.93	3.3
49432.1204	0.109	2.33	2.8	49452.0429	−0.217	2.18	2.7	49630.9529	−0.411	1.53	2.5	49660.9963	−0.398	1.17	7.1	49760.1776	0.104	2.05	3.4
49432.1234	0.102	2.35	3.1	49452.0621	−0.232	2.31	3.0	49630.9711	−0.404	1.46	2.5	49661.0434	−0.409	1.11	7.1	49778.9780	−0.336	1.35	2.6
49432.1439	0.087	2.48	4.2	49452.0820	−0.249	2.43	2.6	49630.9890	−0.405	1.39	2.4	49661.0709	−0.394	1.09	6.1	49779.0185	−0.324	1.49	2.7
49432.1472	0.095	2.50	4.7	49452.1177	−0.258	2.64	2.7	49631.0071	−0.404	1.34	2.6	49661.1374	−0.409	1.09	6.1	49779.0570	−0.308	1.65	2.7
49432.1594	0.072	2.57	4.2	49452.1363	−0.275	2.72	3.5	49631.0271	−0.405	1.28	2.7	49661.1646	−0.396	1.10	6.9	49784.1108	−0.120	2.04	4.3
49432.1629	0.066	2.59	4.3	49452.1572	−0.276	2.79	3.5	49631.0394	−0.402	1.25	2.3	49711.1248	−0.391	1.24	4.6	49784.1158	−0.131	2.07	4.3
49432.1825	0.047	2.69	4.0	49452.1712	−0.312	2.81	2.9	49631.0574	−0.402	1.21	2.4	49711.1282	−0.404	1.25	4.8				
49432.1864	0.050	2.70	4.0	49452.1908	−0.316	2.81	3.3	49657.8671	0.057	1.58	3.6	49711.1314	−0.393	1.26	5.0				

Table 5. Absolute Strömgren photometry of the programme stars. (Values for *IUE* phases.) The quoted total errors are the quadratic sums of the internal and transformation uncertainties.

Date	V	$(b-y)$	$(u-b)$	$(v-b)$	m_1	c_1	Weight
HV 982							
1995 Sep 18	14.719	0.002	0.131	0.010	0.008	0.111	0.5
1995 Sep 19	14.670	−0.074	0.101	0.059	0.133	−0.017	1
1997 Jun 01	14.621	0.007	0.082	−0.059	−0.066	0.201	0.5
1997 Jun 05	14.696	0.097	−0.115	−0.092	−0.189	0.070	1
Weighted mean	14.679	0.009	0.031	−0.019	−0.028	0.070	
Internal error	±0.018	±0.040	±0.060	±0.038	±0.077	±0.043	
Total error	±0.026	±0.041	±0.062	±0.039	±0.078	±0.045	
HV 1620							
1995 Sep 18	14.489	−0.045	0.037	0.013	0.058	0.011	0.5
1995 Sep 19	14.459	0.019	0.017	0.042	0.023	−0.067	1
1995 Oct 25	14.465	0.022	0.032	0.044	0.022	−0.056	1
Weighted mean	14.467	0.007	0.027	0.037	0.030	−0.047	
Internal error	±0.008	±0.019	±0.006	±0.009	±0.010	±0.021	
Total error	±0.022	±0.021	±0.015	±0.013	±0.016	±0.026	
HV 2241							
1995 Sep 18	13.503	0.006	−0.015	0.060	0.054	−0.135	0.5
1995 Oct 25	13.492	0.003	−0.038	0.046	0.043	−0.130	1
Weighted mean	13.496	0.004	−0.030	0.051	0.047	−0.132	
Internal error	±0.005	±0.001	±0.009	±0.005	±0.004	±0.001	
Total error	±0.022	±0.008	±0.017	±0.011	±0.013	±0.016	

Table 4. Absolute VI_C photometry of the programme stars. (Values for *IUE* phases.) The quoted total errors are the quadratic sums of the internal and transformation uncertainties.

Date	V	I_C	$(V-I_C)$	Weight
HV 982				
1994 Dec 26	14.599	14.764	−0.165	1
1994 Dec 26	14.602	14.741	−0.140	1
1995 Feb 12	14.621	14.711	−0.092	1
1995 Feb 12	14.624	14.716	−0.091	1
Weighted mean	14.612	14.733	−0.122	
Internal error	±0.011	±0.017	±0.028	
Total error	±0.016	±0.035	±0.043	
HV 1620				
1994 Dec 26	14.501	14.438	0.063	1
1994 Dec 26	14.502	14.373	0.130	1
1995 Feb 12	14.443	14.376	0.063	1
1995 Feb 12	14.511	14.373	0.139	1
1995 Sep 03	14.441	14.444	−0.001	1
1995 Sep 03	14.432	14.444	−0.015	1
1995 Oct 23	14.486	14.516	−0.031	1
1995 Oct 23	14.505	14.528	−0.023	1
Weighted mean	14.481	14.437	−0.041	
Internal error	±0.025	±0.031	±0.034	
Total error	±0.028	±0.044	±0.047	
HV 2241				
1994 Dec 26	13.497	13.471	0.025	1
1994 Dec 26	13.500	13.453	0.047	1
1995 Feb 12	13.509	13.509	−0.003	1
1995 Feb 12	13.506	13.500	0.007	1
1995 Sep 02	13.508	13.517	−0.008	1
1995 Sep 02	13.514	13.519	−0.006	1
1995 Sep 03	13.524	13.515	0.011	1
1995 Sep 03	13.524	13.512	0.009	1
Weighted mean	13.510	13.500	0.010	
Internal error	±0.005	±0.012	±0.009	
Total error	±0.013	±0.033	±0.034	

3 ANALYSIS

3.1 Ephemerides

We have derived new ephemerides for our programme stars. A simple formulation suffices since the light curves show no evidence of eccentricity. For each star, times and uncertainties of a representative primary minimum during the period of our photometry were obtained from analysis with the WD code. We derived the period of HV 2241 via error-weighted linear regression of our minimum along with the one adopted in Davidge's (1987) ephemeris (both of which have uncertainties of ∼80 s) and the 12 minima between 1896 and 1949 reported by Gaposhkin (1977). For the Gaposhkin timings, we adopted an uncertainty of 90 min, which we consider representative based on analysis of other systems (Watson et al. 1992, Tobin et al. 1993a) and found that despite the long temporal baseline, their effect on the derived period was slight. Our new ephemeris for HV 2241 is:

$$\begin{array}{rcl} \text{Time of} \\ \text{primary} \\ \text{minimum} \end{array} = \begin{array}{l} \text{HJD } 2449477.7285 + 4.3426241 \times E. \\ \pm\ 0.0009 \pm 0.0000016 \end{array}$$

For HV 1620, however, it is less clear what uncertainty to adopt for the epoch of the minimum in the ephemeris reported by Payne-Gaposchkin & Gaposchkin (1966): a 45-minute error gives this minimum in 1947 as much importance in the period determination as the minimum in 1985 adopted by Davidge (1988), which has an uncertainty of 10 min. After regressing the data in various ways, we adopted the following ephemeris for HV 1620 as representative of all the available observations:

$$\begin{array}{rcl} \text{Time of} \\ \text{primary} \\ \text{minimum} \end{array} = \begin{array}{l} \text{HJD } 2449345.7477 + 3.62642 \times E. \\ \pm\ 0.0004 \pm 0.00001 \end{array}$$

Table 6. Flux calibrations for *uvby* and Cousins *UBVRI* bandpasses. The numbers represent the extra-atmospheric fluxes (in units of 10^{-9} erg cm^{-2} s^{-1} Å^{-1} or 10^{-11} W m^{-2} nm^{-1}) of a star of zero magnitude in each passband. The *uvby* calibration adopts $y = V$.

	$\bar{\lambda}$ (nm)	**Adopted** $\mathbf{m_{Vega}}$	**Heber et al. (1984)**	**Bessell (1979)**	**Underhill (1981)**	**This work**
u	347	1.442	11.46		12.05	12.40
v	411	0.195	8.42		9.85	8.82
b	467	0.034	5.65		5.74	5.93
y	546	0.030	3.60		3.69	3.75
U	361	0.03	4.16	4.19		4.26
B	441	0.03	6.17	6.60		6.51
V	551	0.03	3.58	3.61		3.71
R	658	0.09		2.25		2.35
I	806	0.07		1.22		1.19

Table 7. Details of the *IUE* low-resolution spectrophotometry.

Star Image	**Exposure start** (UTC)	**Duration** (s)	**Middle** (HJD) **Phase**[a]
HV 1620	1994 Apr 23	5998.5	2449465.9563
SWP 50613	10:07:42		0.1480
HV 2241	1994 Dec 12	2399.2	2449689.7874
SWP 52968	06:33:45		0.8320

[a]Calculated according to the ephemerides given in Section 3.1.

3.2 Interstellar reddening and extinction

The optical reddening laws of the Galaxy and both Magellanic Clouds are similar (e.g. Bouchet et al. 1985) and the Kurucz model atmospheres indicate that the optical colours of B stars are insensitive to metallicity. We therefore determined the total reddening $E(b-y)$ to each target star in the standard way in the $(b-y)/c_1$ diagram (Figure 5). For this, the observed composite colours at the *IUE* phases were deconvolved to the colours of the individual stars using light ratios yielded by the WD code.

Table 8. $E(B-V)$ reddening values.

Method	**Resolution**	**HV 1620**	**HV 2241**
Foreground			
H I (Schwering & Israel 1991)	48′	0.10 ±0.01	0.10 ±0.01
H I (McGee & Newton 1982, Bessell 1991)	15′	0.076 ±0.02	
Stellar photometry (Oestreicher et al. 1995)	10′		0.066 ±0.02
Adopted		0.09 ±0.02	0.085 ±0.02
Total to star			
$(b-y)/c_1$[a] (Crawford 1978)		0.168 ±0.035	0.174 ±0.020
To infinity			
H I (McGee & Newton 1982, Bessell 1991)	15′	0.174 ±0.035	
H I (McGee & Milton 1966, Koornneef 1982)	14′.5		0.187 ±0.035

[a]Converted to $E(B-V)$ values using the relation $E(B-V) = E(b-y)/0.74$ (Crawford 1975).

The amount of foreground reddening in the direction of the Clouds has been controversial. Some authors (e.g. McNamara & Feltz 1980) have adopted small values–$E(B-V) \simeq 0.03$–whereas more recent authors, and particularly Bessell (1991), have argued for significantly larger values.

We find the arguments for larger values more convincing. We have determined the foreground reddening for our programme stars in various ways. For both stars, we have read values from the coarse-resolution (48 arcmin), H I-derived maps given by Schwering & Israel (1991). For HV 1620 we have also integrated the H I emission profile presented by McGee & Newton (1982) over the range of Galactic velocities and used the Galactic $N(\mathrm{H\,I})/E(B-V)$ ratio determined by Bohlin, Savage & Drake (1978). These H I data have a resolution of 15 arcmin. For HV 2241 we have used the LMC foreground reddening map presented by Oestreicher, Gochermann & Schmidt-Kaler (1995), which is based on *UBV* photometry of foreground stars. This map has a spatial resolution of 10 arcmin.

The foreground reddenings from different resolutions are essentially concordant. They are presented in Table 8 along with the average values adopted for the analysis that follows.

Table 8 also presents values for the reddening to infinity. For HV 1620, the value derives from in addition integrating the McGee & Newton profile over SMC velocities and using Bessell's (1991) SMC $N(\mathrm{H\,I})/E(B-V)$ ratio appropriate for a high value of the foreground reddening. For HV 2241, McGee & Milton (1966) present H I profiles only over the range of LMC velocities. These were integrated, converted to $E(B-V)$ values using the LMC $N(\mathrm{H\,I})/E(B-V)$ ratio given by Koornneef (1982) and added to the adopted foreground reddening. The similarity of the total reddenings to the programme stars and to infinity suggests that both HV 1620 and HV 2241 are located towards the rear of the gas in their respective Clouds.

3.3 Light-curve solutions

All light curve analysis of HV 1620 and HV 2241 was carried out with the Wilson & Devinney synthetic light curve code. The WD code permits the simultaneous solution of multiple light and/or radial-velocity curves and includes the effects of tidally (and rotationally) distorted components by modelling the surface of the stars as Roche equipotential surfaces. We used a modified version of the WD code incorporating the atmosphere subroutine of the Calgary group (Milone, priv. comm.) which uses Kurucz model atmospheres (Kurucz 1993) rather than black bodies or the Carbon-Gingerich atmosphere models as in standard versions of the WD code.

The investigations by Davidge (1987, 1988) indicated both systems to be in, or at least very close to, semi-detached configurations, thus warranting use of the WD code, rather than alternative simpler but faster codes. The semi-detached configuration with the secondary component filling its Roche lobe was quickly confirmed as the most appropriate mode for both systems.

Davidge detected the O'Connell effect in the light curve of HV 2241 in the sense that the maximum of light following primary minimum is slightly brighter than the maximum following secondary minimum. We confirm this obser-

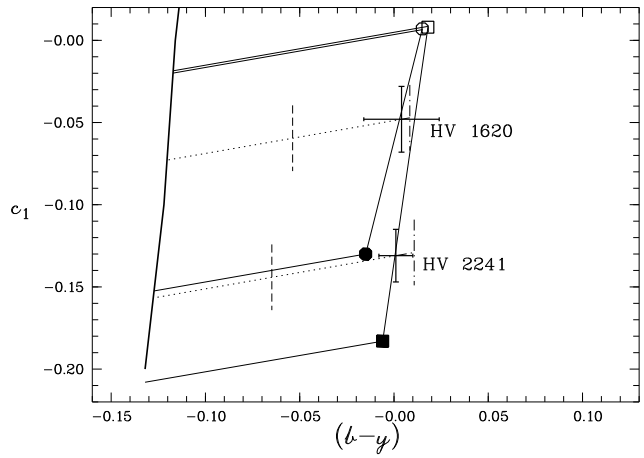

Figure 5. Total reddenings to HV 1620 and HV 2241. The total reddening is derived from the displacement of the colours of the components of each eclipsing binary from the empirical $(b-y)_0$ vs c_0 relation for B stars (Crawford 1978, heavy line) and a reddening ratio $E(c_1)/E(b-y) = 0.2$ (Crawford 1975). Also indicated are the foreground reddenings (dashed lines) and reddenings to infinity (dot-dash lines), as explained in the text. The adopted reddenings are HV 1620: $E(b-y) = 0.124 \pm 0.027$; HV 2241: $E(b-y) = 0.129 \pm 0.015$ and for stars this hot these reddenings differ negligibly from the values that would be obtained using the composite photometry (represented by the error bar crosses and dotted lines).

vation, finding a brightness difference of ∼0.05 mag. in u and ∼0.03 mag. in the other bandpasses. Furthermore, we have detected a similar but smaller effect in the light curve of HV 1620 (∼0.02 mag. in u and ∼0.01 mag. in the other bands). The cause of the O'Connell effect in hot stars is uncertain. We have modelled it arbitrarily by placing 'hot spots' on the equators of the primary components so as to be visible at the quadratures following primary minima. Clearly no analysis of HV 1620, HV 2241, or any other binary exhibiting an O'Connell effect can be considered definitive until its physical mechanism is identified and modelled. However, if the amplitude of the O'Connell effect is indicative of the uncertainty in present model predictions of the systems' radiative surface fluxes, the effect in the error budget for the derived distances will only be a few percent, small compared to the perhaps 7 per cent distance accuracy claimed attainable with eclipsing binary stars (Giménez et al. 1994).

Using our six-colour, CCD light curves we sought to optimise the following parameters with the WD Differential Corrections program (`DC`): the orbital phase offset, the inclination (i), the mass ratio (q), the effective temperature of the secondary component ($T_{\rm eff,2}$) [for a given primary-component effective temperature, $T_{\rm eff,1}$], the surface potential of the primary component (Ω_1) and the radius of the hot spot (where appropriate). Kurucz models with abundances $[m/{\rm H}] = -0.5$ were used for HV 1620 and $[m/{\rm H}] = -0.3$ for HV 2241. Limb-darkening coefficients were interpolated in tables calculated from the Kurucz models and the photometric system responses. Gravity-darkening exponents and bolometric albedoes were set to theoretical values for radiative envelopes. Axial-to-orbital rotation rates were set to unity. The orbital inclination of the binary system is well defined by the absolute depths of the the two eclipses. Wilson (1994) makes a convincing argument for the mass ratio being well defined by the light curve for the case of semi-detached systems. Given the effective temperature of one component, the corresponding effective temperature of the other is well defined by the relative depths of the two eclipses; however there is little information in the light curves regarding the absolute temperature scale, which must be determined from other information. Finally, in the semi-detached mode, the surface potential of the lobe-filling component is defined as the critical Roche potential and is therefore not optimized but calculated for each iteration in terms of the other input parameters. We set the hot spot to be 10 percent hotter than its surroundings leaving only its radius to be solved for.

In each iteration we allowed `DC` to adjust all parameters to be optimized rather than breaking the parameter set up into 'multiple subsets' as suggested by Wilson & Biermann (1976). There were significant correlations between certain of the parameters, in particular the inclination and the surface potential of the primary, but as Wilson & Biermann point out, for the usual method of adjusting all parameters simultaneously, 'convergence is adversely affected not so much by a few very high correlations as by the presence of many high correlations'.

Initially, we judged iterations to have converged once the suggested parameter corrections for all adjusted parameters were smaller than their respective standard errors for two consecutive iterations. Continuing iterations did not generally lead to 'utterly negligible' suggested parameter corrections. Therefore, to test the uniqueness of our solutions we began iterations from several different initial parameter sets which differed substantially from each other and the 'final' solution. A consistent solution was eventually reached from all initial parameter sets, although not necessarily at the first instance at which two consecutive iterations had suggested parameter corrections all smaller than their standard errors. Once the iterations arrived at the final solutions, the parameters 'bounced around' with an amplitude comparable to their standard errors as reported by the `DC` program.

To determine effective temperatures we have chosen to match observed and theoretical flux distributions because these are more directly related to effective temperature than, say, spectral types. We note that the 'infra-red flux method,' which has been claimed to minimize the effects of interstellar reddening in temperature determinations, holds no advantage of accuracy over flux fitting (Tobin 1983).

We wrote a computer program derived from the WD code to generate theoretical spectral flux distributions for a range of solution parameter sets corresponding to a range of values of $T_{\rm eff,1}$. We reddened the theoretical fluxes by applying the Galactic interstellar extinction law of Howarth (1983) for the foreground extinction. For the interstellar extinction in the Clouds we adopted Howarth's Galactic law for wavelengths shorter than 278 nm and 346 nm for the LMC and the SMC respectively. For the ultraviolet extinction in the Clouds we adopted Fitzpatrick's (1986) 'Average LMC curve' for the LMC and interpolated from the table provided by Prévot et al. (1984) for the SMC. We took $R = A_V/E(B-V) = 3.1$ for the Galaxy (Howarth 1983) and the LMC (Koornneef 1982) and $R = 2.7$ for the SMC (Bouchet et al. 1985).

Comparison of these reddened theoretical fluxes to the

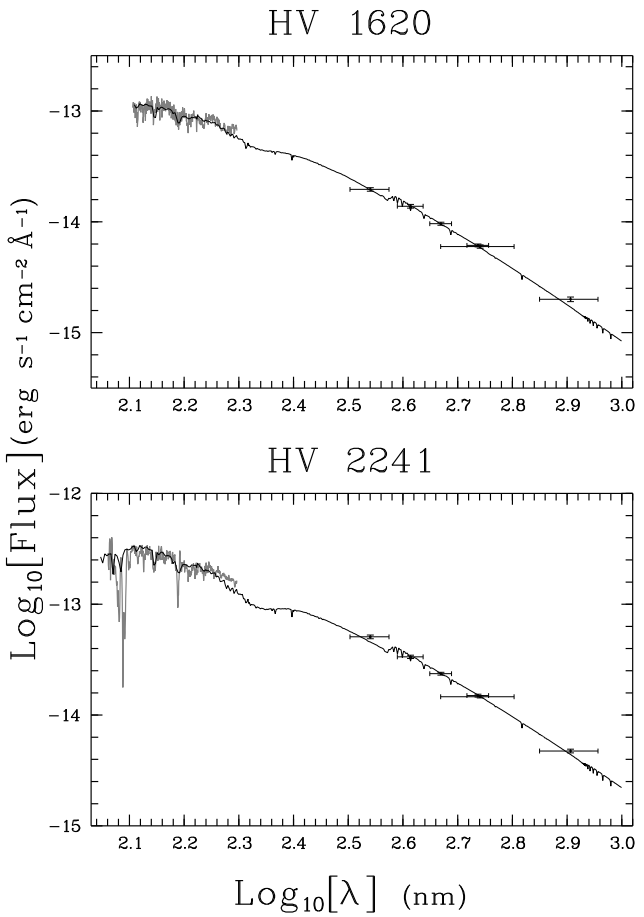

Figure 6. Reddened theoretical spectral fluxes for the adopted effective temperatures (Table 9) overplotted on the observed *IUE* uv spectrophotometry (∼5 per cent uncertainty) and calibrated *uvbyV* I_C fluxes (vertical error bars. The horizontal bars indicate the width of each bandpass.) The I_C flux was excluded from the flux fit for HV 1620 because the poor I_C light-curve fit (Fig. 4 suggests contamination by third light.)

observed spectral flux distributions (the *uvbyV* I_C photometry plus the *IUE* spectrophotometry, see Figure 6) allowed estimation of the effective temperatures of the two components of each system (see Table 9). By eye, the uncertainty in the $T_{\rm eff,1}$ estimates, for a given combination of reddenning and interstellar extinction laws, is of the order of 1 000 K due to the relatively weak dependence of flux gradient over the observed spectral range ($\lambda\lambda$∼115–800 nm) for these very hot stars. We have estimated the total uncertainty in the $T_{\rm eff}$ estimates by determining the temperatures corresponding to the extreme values of the reddenings and, to allow for the considerable uncertainty that still surrounds the extinction laws in the Clouds, by using various combinations of the interstellar extinction laws, e.g. reddening the theoretical fluxes using the Galactic extinction law for both foreground and Cloud extinction.

Results of the light curve analysis are presented in Table 9. Figure 7 illustrates the extent to which the systems are filling their Roche lobes. Figure 4 presents representative light-curve fits and residuals.

Table 9. Final values for the optimized parameters of HV 1620 and HV 2241 from the analysis of the light curves and absolute photometry. Uncertainties have been estimated after consideration of the standard errors reported by the WD program, the rms scatter amongst ensembles of solutions according to the adopted convergence criterion (see text), and differences between solutions for models both with and without a spot to model the O'Connell effect (see text). The uncertainty in the effective temperatures is dominated by the uncertainty in the reddening. For a given value of $T_{\rm eff,1}$ the uncertainty in $T_{\rm eff,2}$ is of the order of 100 K.

Parameter	Value
HV 1620	
Inclination, i	$77\overset{\circ}{.}10 \pm 0\overset{\circ}{.}4$
Eccentricity, e	0 (adopted)
Mass ratio, q	0.68 ± 0.03
Effective Temperature, $T_{\rm eff,1}$	$33\,000 \pm 4\,500$ K
$T_{\rm eff,2}$	$24\,400 \pm 3\,500$ K
Surface Potential, Ω_1	5.89 ± 0.10
Ω_2	3.21 ± 0.06
HV 2241	
Inclination, i	$85\overset{\circ}{.}3 \pm 0\overset{\circ}{.}6$
Eccentricity, e	0 (adopted)
Mass ratio, q	0.53 ± 0.01
Effective Temperature, $T_{\rm eff,1}$	$27\,000 \pm 3\,000$ K
$T_{\rm eff,2}$	$20\,200 \pm 1\,500$ K
Surface Potential, Ω_1	3.25 ± 0.03
Ω_2	2.93 ± 0.02

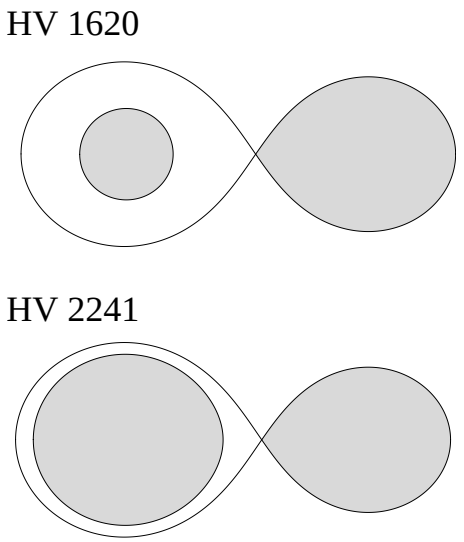

Figure 7. Representative schematics of the surfaces of HV 1620 and HV 2241 in the plane perpendicular to the orbital plane. For HV 1620, the primary component (on the left) is well inside its critical Roche lobe while for HV 2241 the primary is much closer to filling its Roche lobe. The secondary component fills its Roche lobe in both stars.

3.4 Fundamental parameters

Radial-velocity curves are needed to obtain masses, radii and distances for HV 1620 and HV 2241. The radial-velocity curves presented by Niemela & Bassino (1994) were obtained with a 1-metre telescope. Although Niemela & Bassino give few details about their procedure, they must have used

strong lines, i.e. hydrogen and helium. Andersen, Clausen & Nordström (1980) have shown that the use of hydrogen and helium lines can lead to errors between 10 and 40 per cent in the derived masses. Fundamental parameters derived from the Niemela & Bassino velocities can thus only be illustrative of the nature of HV 1620 and HV 2241.

Nevertheless we have included quadrature radial velocities from Niemela & Bassino in our WD analysis. The effect on the derived mass ratios is negligible because of the small number of measures and their large scatter. No trends are visible in the velocity residuals (Figure 4). Photometrically-determined mass ratios fall within the much larger uncertainties of the spectroscopic values determined by Niemela & Bassino.

The resulting semi-major axes for HV 1620 and HV 2241 are $\sim$30 and $\sim$40 $R_\odot$, respectively. The primary and secondary masses and radii are $\sim$20 $M_\odot$, $\sim$15 $M_\odot$, $\sim$6 $R_\odot$ and $\sim$11 $R_\odot$ for HV 1620, and $\sim$35 $M_\odot$, $\sim$20 $M_\odot$, $\sim$16 $R_\odot$ and $\sim$14 $R_\odot$ for HV 2241. The distance moduli are $\sim$18.6 and $\sim$18.5. If the mass errors are 40 per cent, the uncertainties in the semi-major axes and radii are $\sim$15 per cent. The uncertainties in the distance moduli are $\sim$0.5 mag.; these include a non-negligible contribution from the uncertainty in the effective temperatures.

4 DISCUSSION

Eclipsing binaries in the Magellanic Clouds merit study both because of the information they may yield on stellar evolution at low metallicity and because they may give distances to these cosmologically-important galaxies. The highest quality data are a prerequisite for useful results.

For HV 1620 and HV 2241 we have presented much better differential photometry and better absolute photometry than in earlier papers in the series. However for determination of accurate temperatures better absolute photometry is still required. The disaccord between V magnitudes obtained with y and V filters is disquieting. More calibration observations would certainly be desirable. The disagreement seems to increase with crowding, but if so, it is puzzling that the correction for nearby field stars results in such good differential photometry (see also Paper VI).

We have found that effective temperature determinations are also affected substantially by variations in the interstellar reddening internal to the Clouds. Further study of the uv-visible reddening laws is warranted. Several parameters may be necessary to characterize the extinction curve in any given direction. It remains to be seen whether such parameters can be obtained e.g. via stellar spectrophotometry over a broad wavelength range such can be obtained with the HST Faint Object Spectrograph, and whether the effects of extinction and stellar continuum slope can be disentangled accurately enough.

HV 1620 and HV 2241 are massive close binaries with secondaries that fill their Roche lobes. Even though precise understanding of their evolutionary state may be difficult because of the effects of mass exchange and tidal distortion, it may be that these systems can act as accurate distance indicators. Though its effect is probably small, it would nevertheless be preferable to use systems which do not exhibit the O'Connell effect, which is not understood physically. Thus detached systems are to be preferred both for tests of stellar evolution outside the Galaxy and as extragalactic distance indicators.

To obtain fundamental parameters accurate radial-velocity curves are required. Methods for avoiding systematic errors have been discussed by e.g. Harries, Hilditch & Hill (1997).

5 ACKNOWLEDGMENTS

We thank: A.C. Gilmore and M. Zambri for assisting in some of the calibration observations; P.M. Kilmartin and A.C. Gilmore for obtaining the accurate coordinates essential for *IUE* pointing; Dr R.L. Kurucz for providing CD-ROMs of his model atmospheres; Dr C. Imhoff and colleagues for reprocessing *IUE* images; Dr M. Oestreicher for providing the computerized version of the LMC foreground reddening map; Dr R. Wilson for providing his synthetic light-curve code; Dr E.F. Milone for providing his `ATM` subroutine to incoprorate the Kurucz atmosphere models into the Wilson & Devinney code; Dr T. Davidge for providing tabulations of his light curves for HV 1620 and HV 2241; and Drs J.-V. Clausen & G. Hill for their many valuable comments made during the preparation of this paper.

JDP would like to acknowledge the financial support provided by the Department of Physics & Astronomy, University of Canterbury, and the Marsden Fund of New Zealand.

This research has made use of the SIMBAD database operated at CDS, Strasbourg, France.

REFERENCES

Andersen J., 1991, A&AR, 3, 91
Andersen J., Clausen J.V., Nordström B., 1980, in Plavek M.J., Popper D.M., Ulrich R.K., eds, Proc. IAU Symp. 88, Close binary stars: Observations and interpretation. Reidel, Dordrecht, p. 81
Banse K., Ponz D., Ounnas Ch., Grosbøl P. Warmels R., 1987, in Robinson L.B. ed, Instrumentation for Ground-Based Optical Astronomy: Present and Future. Ninth Santa Cruz Summer Workshop in Astronomy and Astrophysics. Springer-Verlag, New York, p. 431
Bessell M.S., 1979, PASP, 91, 589
Bessell M.S., 1990, PASP, 102, 1181
Bessell M.S., 1991, A&A, 242, L17
Bessell M.S., 1995, PASP, 107, 672
Bessell M.S., Wickramasinghe D.T., 1978, MNRAS, 182, 275
Bohlin R.C., Savage B.D., Drake J.F., 1978, ApJ, 224, 132
Bouchet P., Lequeux J., Maurice E., Prévot L., Prévot-Burnichon M.L., 1985, A&A, 149, 330
Buonanno R., Iannicola G., 1989, PASP, 101, 294
Castelli F., Kurucz R.L., 1994, A&A, 281, 817
Cousins A.W.J., 1987, S. Afr. Astron. Obs., Circ., 11, 93
Crawford D.L., 1975, PASP, 87, 481
Crawford D.L., 1978, AJ, 83, 48
Crawford D.L., Barnes J.V., Gibson J., Golson J.C., Perry C.L., Crawford M.L., 1972, A&AS, 5, 109
Davidge T.J., 1987, AJ, 94, 1169
Davidge T.J., 1988, AJ, 95, 731
Djorgovski S., 1984, in Borucki W.J., Young A., eds, Proceedings of the Workshop on Improvements to Photometry, NASA CP-2350, p. 152

Duncan S.P.R., Tobin W., Watson R.D., Gilmore A.C., 1993, MNRAS, 265, 189
ESA, 1997, The Hipparcos and Tycho Catalogues, Vol. 1, ESA SP-1200
Etzel P.B., 1981, in Carling E.B., Kopal Z., eds, Photometric and Spectroscopic Binary Systems, Reidel, Dordrecht, p. 111
Etzel P.B., 1993, in Milone E.F., ed, Light Curve Modeling of Eclipsing Binary Stars, Springer-Verlag, New York, p. 113
Fitzpatrick E.L., 1986, AJ, 92, 1068
Gaposhkin S.I., 1977, Smithson. Astrophys. Obs. Spec. Rep., No. 380
Garhart M.P., 1992, IUE NASA Newsletter, 48, 98
Giménez A., Clausen J.V., Guinan E.F., Maloney F.P., Bradstreet D.H., Storm J., Tobin W., 1994, Exp. Astron., 5, 181
Graham J.A., 1972, AJ, 77, 144
Graham J.A., 1982, PASP, 94, 244
Graham J.A., Slettlebak A., 1973, AJ, 78, 295
Grosbøl P., 1989, Rev. Modern Astr., 2, 242
Guinan E.F., Bradstreet D.H., DeWarf L.E., 1996, in Milone E.F., Mermilliod J-C., eds, The Origins, Evolution, and Destinies of Binary Stars in Clusters, ASP, San Francisco, p. 196
Harries T.J., Hilditch R.W., Hill, G., 1997, MNRAS, 285, 277
Harris W.E., Fitzgerald M.P., Reed B.C., 1981, PASP, 93, 507
Heber U., Hunger K., Jonas G., Kudritzki R.P., 1984, A&A, 130, 119
Herczeg T.J., 1982, in Kopal Z., Rahe J., eds, Binary and Multiple Stars as Tracers of Stellar Evolution. Reidel, Dordrecht, p. 145
Hilditch R.W., 1996, in Milone E.F., Mermilliod J-C., eds, The Origins, Evolution, and Destinies of Binary Stars in Clusters, ASP, San Francisco, p. 207
Howarth I.D., 1983, MNRAS, 203, 301
Johnson H.L., 1965, ApJ, 141, 923
Kilkenny D., 1977, MNRAS, 181, 611
Kilkenny D., Hill P.W., 1975, MNRAS, 173, 625
Kilkenny D., Hill P.W., Brown A., 1977, MNRAS, 178, 123
Kilkenny D., Laing J.D., 1992, MNRAS, 255, 308
Kilkenny D., Menzies J.W., 1989, S. Afr. Astron. Obs., Circ., 13, 25
Koornneef J., 1982, A&A, 107, 247
Kurucz R.L., 1993, in Milone E.F., ed, Light Curve Modeling of Eclipsing Binary Stars. Springer-Verlag, New York, p. 93
Lamla E., 1982, in Schaifers K., Voigt H.H., eds, Landolt-Börnstein Neue Serie, Gp IV, Vol. 2b. Springer-Verlag, Berlin, p. 52
Landolt A.U., 1992, AJ, 104, 340
Lubow S.H., Shu, F.H., 1975, ApJ, 198, 383
Manfroid J., 1995, A&AS, 113, 587
Matsushima S., 1969, ApJ, 158, 1137
McGee R.X., Milton J.A., 1966, Australian J. Phys., Astrophys. Suppl., No. 2
McGee R.X., Newton L.M., 1982, Proc. Australian Astr. Soc. 4, 308
McNamara D.H., Feltz K.A. Jr., 1980, PASP, 92, 587
Mégessier C., 1995, A&A, 296, 771
Menzies J.W., Cousins A.W.J., Banfield R.M., Laing J.D., 1989, S. Afr. Astron. Obs., Circ., 13, 1
Menzies J.W., Marang F., Westerhuys J.E., 1990, S. Afr. Astron. Obs., Circ., 14, 33
Nichols J.S., Linsky J.L., 1996, AJ, 111, 517
Niemela V.S., Bassino L.P., 1994, ApJ, 437, 332
Olson E.C., 1974, PASP, 86, 80
Oestreicher M.O., Gochermann J., Schmidt-Kaler T., 1995, A&AS, 112, 495
Paczyński B., 1997, in Ferlet R., Maillard J.-P., Rabam B., eds, Variable Stars and the Astrophysical Returns of Microlensing Surveys. Editions Frontières, Gif-sur-Yvette, p. 309
Payne-Gaposchkin C., Gaposchkin S., 1966, Smithson. Contrib. Astrophys., 9, 1
Prévot M.L., Lequeux J., Maurice E., Prévot L., Rocca-Volmerange B., 1984, A&A, 132, 389
Pritchard J.D., 1997, Ph.D. thesis, University of Canterbury, New Zealand
Russell H.N., 1956, Vistas Astron., 2, 1177
Schwering P.W.B., Israel, F.P., 1991, A&A, 246, 231
Stetson P.B., 1987, PASP, 99, 191
Stoy R., 1966, Ann. Cape Obs., 21
Tobin, W., 1983, A&A, 125, 168
Tobin W., 1992, Southern Stars, 34, 421
Tobin W., 1993, in Butler C.J., Elliott I., eds, Stellar Photometry: Current Techniques and Future Developments. Cambridge University Press, Cambridge, p. 304
Tobin W., Duncan S.P.R., West S.R.D., Gilmore A.C., 1993a, MNRAS, 260, 777
Tobin W., Kershaw G.M., Ritchie R.A., Ma L., Graham G.J., Hemmingsen S.B., 1993b, in Elliott I., Butler C.J., eds, Poster papers on stellar photometry. DIAS, Dublin, p. 153
Underhill A.B., 1981, ApJ, 244, 963
Watson R.D., West S.R.D., Tobin W., Gilmore A.C., 1992, MNRAS, 258, 527
West S.R.D., Tobin W., Gilmore A.C., 1992, MNRAS, 254, 419
Wilson R.E., 1979, ApJ, 234, 1054
Wilson R.E., 1994, PASP, 106, 921
Wilson R.E., Biermann P., 1976, A&A, 48, 349

This paper has been produced using the Royal Astronomical Society/Blackwell Science LaTeX style file.